

9. OVERVIEW OF TITAN-I DESIGN

Farrokh Najmabadi

Steven P. Grotz

Clement P. C. Wong

Contents

9.1.	INTRODUCTION	9-1
9.2.	CONFIGURATION	9-7
9.3.	MATERIALS	9-15
9.4.	NEUTRONICS	9-19
9.5.	THERMAL AND STRUCTURAL DESIGN	9-23
9.6.	MAGNET ENGINEERING	9-28
9.7.	POWER CYCLE	9-32
9.8.	DIVERTOR ENGINEERING	9-33
9.9.	TRITIUM SYSTEMS	9-40
9.10.	SAFETY DESIGN	9-43
9.11.	WASTE DISPOSAL	9-46
9.12.	MAINTENANCE	9-48
9.13.	SUMMARY AND KEY TECHNICAL ISSUES	9-53
	REFERENCES	9-61

9. OVERVIEW OF TITAN-I DESIGN

9.1. INTRODUCTION

The TITAN research program is a multi-institutional [1] effort to determine the potential of the reversed-field-pinch (RFP) magnetic fusion concept as a compact, high-power-density, and “attractive” fusion energy system from economics (cost of electricity, COE), safety, environmental, and operational viewpoints.

In recent reactor studies, the compact reactor option [2-5] has been identified as one approach toward a more affordable and competitive fusion reactor. The main feature of a compact reactor is a fusion power core (FPC) with a mass power density in excess of 100 to 200 kWe/tonne. Mass power density (MPD) is defined [2] as the ratio of the net electric power to the mass of the FPC, which includes the plasma chamber, first wall, blanket, shield, magnets, and related structure. The increase in MPD is achieved by increasing the plasma power density and neutron wall loading, by reducing the size and mass of the FPC through decreasing the blanket and shield thicknesses and using resistive magnet coils, as well as by increasing the blanket energy multiplication. A compact reactor, therefore, strives toward a system with an FPC comparable in mass and volume to the heat sources of alternative fission power plants, with MPDs ranging from 500 to 1000 kWe/tonne and competitive cost of energy.

Other potential benefits for compact systems can be envisaged in addition to improved economics. The FPC cost in a compact reactor is a small portion of the plant cost and, therefore, the economics of the reactor will be less sensitive to changes in the unit cost of FPC components or the plasma performance. Moreover, since a high-MPD FPC is smaller and cheaper, a rapid development program at lower cost should be possible, changes in the FPC design will not introduce large cost penalties, and the economics of learning curves can be readily exploited throughout the plant life.

The RFP has inherent characteristics which allow it to operate at very high mass power densities. This potential is available because the main confining field in an RFP is the poloidal field, which is generated by the large toroidal current flowing in the plasma. This feature results in a low field at the external magnet coils, a high plasma beta, and a very high engineering beta (defined as the ratio of the plasma pressure to the square of the magnetic field strength at the coils) as compared to other confinement schemes.

Furthermore, sufficiently low magnetic fields at the external coils permit the use of normal coils while joule losses remain a small fraction of the plant output. This option allows a thinner blanket and shield. In addition, the high current density in the plasma allows ohmic heating to ignition, eliminating the need for auxiliary heating equipment. Also, the RFP concept promises the possibility of efficient current-drive systems based on low-frequency oscillations of poloidal and toroidal fluxes and the theory of RFP relaxed states. The RFP confinement concept allows arbitrary aspect ratios, and the circular cross section of plasma eliminates the need for plasma shaping coils. Lastly, the higher plasma densities particularly at the edge, together with operation with a highly radiative RFP plasma, significantly reduce the divertor heat flux and erosion problems.

These inherent characteristics of the RFP [6] allow it to meet, and actually far exceed, the economic threshold MPD value of 100 kWe/tonne. As a result, the TITAN study also seeks to find potentially significant benefits and to illuminate main drawbacks of operating well above the MPD threshold of 100 kWe/tonne. The program, therefore, has chosen a minimum cost, high neutron wall loading of 18 MW/m² as the reference case in order to quantify the issue of engineering practicality of operating at high MPDs. The TITAN study has also put strong emphasis on safety and environmental features in order to determine if high-power-density reactors can be designed with a high level of safety assurance and with low-activation material to qualify for Class-C waste disposal.

An important potential benefit of operating at a very high MPD is that the small physical size and mass of a compact reactor permits the design to be made of only a few pieces and a single-piece maintenance approach will be feasible [7,8]. Single-piece maintenance refers to a procedure in which all of components that must be changed during the scheduled maintenance are replaced as a single unit, although the actual maintenance procedure may involve the movement, storage, and reinstallation of some other reactor components. In TITAN designs, the entire reactor torus is replaced as a single unit during the annual scheduled maintenance. The single-piece maintenance procedure is expected to result in the shortest period of downtime during the scheduled maintenance period because: (1) the number of connects and disconnects needed to replace components will be minimized; and (2) the installation time is much shorter because the replaced components are pretested and aligned as a single unit before commitment to service. Furthermore, recovery from unscheduled events will be more standard and rapid because complete components will be replaced and the reactor brought back on line. The repair work will then be performed outside the reactor vault.

To achieve the design objectives of the TITAN study, the program was divided into two phases, each roughly one year in length: the Scoping Phase and the Design Phase.

The objectives of the Scoping Phase were to define the parameter space for a high-MPD RFP reactor and to explore a variety of approaches to major subsystems. The Design Phase focused on the conceptual engineering design of basic ideas developed during the Scoping Phase with direct input from the parametric systems analysis and with strong emphasis on safety, environmental, and operational (maintenance) issues.

Scoping Phase activities of the TITAN program were reported separately [1]. Four candidate TITAN FPCs were identified during the Scoping Phase:

1. A self-cooled, lithium-loop design with a vanadium-alloy structure;
2. An aqueous, self-cooled "loop-in-pool" design in which the entire FPC is submerged in a pool of water to achieve a high level of passive safety;
3. A self-cooled FLiBe pool design using a vanadium-alloy structure; and
4. A helium-cooled ceramic design with a solid breeder and silicon carbide structure.

Two of the above FPC designs were selected for detail evaluation during the Design Phase because of inadequate resources to pursue all four designs. The choice of which two concepts to pursue was difficult; all four concepts have attractive features. The lithium-loop design promises excellent thermal performance and is one of the main concepts being developed by the blanket technology program. The water-cooled design promises excellent safety features and uses more developed technologies. The helium-cooled ceramic design offers true inherent safety and excellent thermal performance. The molten-salt pool design is the only low-pressure blanket and promises a high degree of passive safety. The lithium-loop (TITAN-I) and the aqueous "loop-in-pool" (TITAN-II) concepts were chosen for detailed conceptual design and evaluation in the Design Phase. The choice was based primarily on the capability to operate at high neutron wall load and high surface heat flux. The choice not to pursue the helium-ceramic and molten-salt designs should in no way denigrate these concepts. Both concepts offer high performance and attractive features when used at lower wall loads; these concepts should be pursued in future design studies.

The operating space of a compact RFP reactor has been examined using a comprehensive parametric systems model which includes the evolving state of knowledge of the physics of RFP confinement and embodies the TITAN-I and TITAN-II engineering approaches (Section 3). Two key figures of merit, the cost of electricity (COE) and mass power density (MPD), are monitored by the parametric systems model and are displayed

in Figure 9.1-1 as functions of the neutron wall loading. Figure 9.1-1 shows that the COE is relatively insensitive to wall loadings in the range of 10 to 20 MW/m², with a shallow minimum at about 19 MW/m². The MPD is found to increase monotonically with the wall load. For designs with a neutron wall load larger than about 10 MW/m², the FPC is physically small enough such that single-piece FPC maintenance is feasible. These considerations point to a design window for compact RFP reactors with neutron wall loading in the range of 10 to 20 MW/m². The TITAN-class RFP reactors in this design window have an MPD in excess of 500 kWe/tonne, and an FPC engineering power density in the range of 5 to 15 MWt/m³; these values represent improvements by factors of 10 to 30 compared with earlier fusion reactor designs. The FPC cost is a smaller portion of the total plant cost (typically about 12%) compared with 25% to 30% for earlier RFP designs [4,5]. Therefore, the unit direct cost (UDC) is less sensitive to related physics and technology uncertainties.

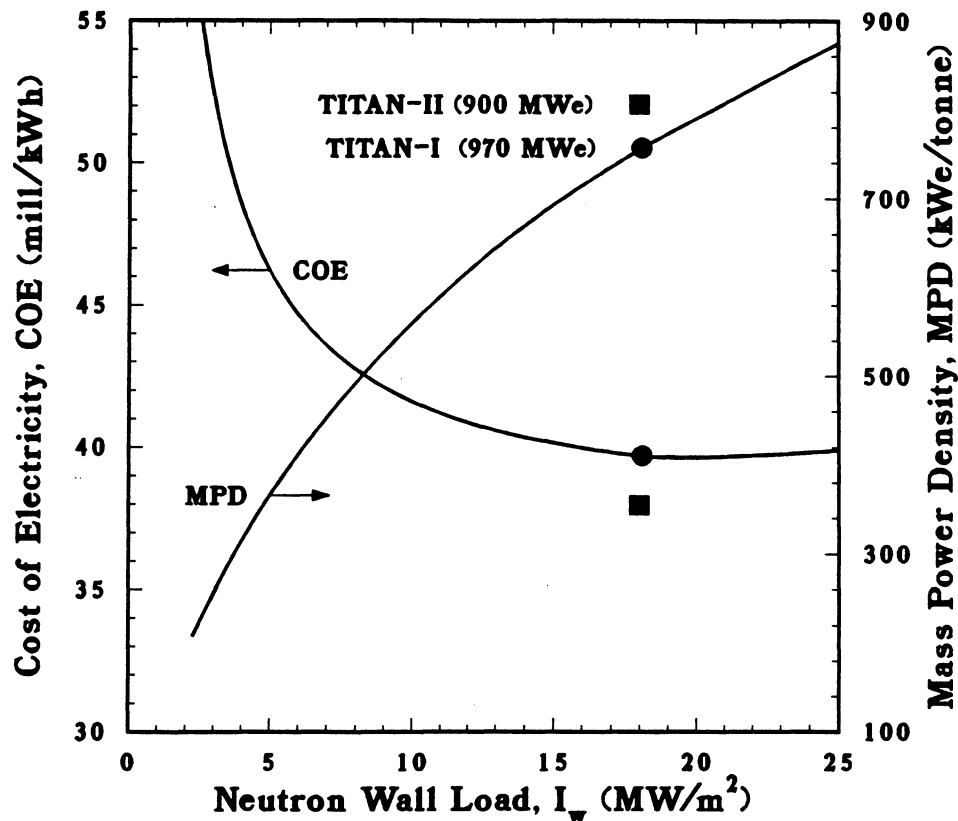


Figure 9.1-1. The COE and MPD as functions of neutron wall loading for the TITAN-class RFP reactors. TITAN-I (filled circle) and TITAN-II (filled squares) reference design points are also shown.

Table 9.1-I.

OPERATING PARAMETERS OF TITAN FUSION POWER CORES

	TITAN-I	TITAN-II
Major radius (m)	3.9	3.9
Minor plasma radius (m)	0.60	0.60
First wall radius (m)	0.66	0.66
Plasma current (MA)	17.8	17.8
Toroidal field on plasma surface (T)	0.36	0.36
Poloidal beta	0.23	0.23
Neutron wall load (MW/m ²)	18	18
Radiation heat flux on first wall (MW/m ²)	4.6	4.6
Primary coolant	Liquid lithium	Aqueous solution
Structural material	V-3Ti-1Si	Ferritic steel 9-C
Breeder material	Liquid lithium	LiNO ₃
Neutron multiplier	none	Be
Coolant inlet temperature (°C)	320	298
First-wall-coolant exit temperature (°C)	440	330
Blanket-coolant exit temperature (°C)	700	330
Coolant pumping power (MW)	48	49
Fusion power (MW)	2301	2290
Total thermal power (MW)	2935	3027
Net electric power (MW)	970	900
Gross efficiency	44%	35%
Net efficiency	33%	30%
Mass power density, MPD (kWe/tonne)	757	806
Cost of electricity, COE (mill/kWh)	39.7	38.0

Near-minimum-COE TITAN-I and TITAN-II design points, incorporating distinct blanket thermal-hydraulic options, materials choices, and neutronics performances have been identified in Figure 9.1-1. The major parameters of the TITAN reactors are summarized in Table 9.1-I. In order to permit a comparison, the TITAN reference design points have similar plasma parameters and wall loadings allowing for certain plasma engineering analyses to be common between the two designs.

The TITAN RFP plasma operates at steady state using oscillating-field current drive (OFCD) to maintain the 18 MA of plasma current. This scheme [9,10] utilizes the strong coupling, through the plasma relaxation process which maintains the RFP profiles [11], between the toroidal and poloidal fields and fluxes in the RFP. Detailed plasma/circuit simulations have been performed which include the effects of eddy currents induced in the FPC (Section 7). The calculated efficiency of the TITAN OFCD system is 0.3 A/W delivered to the power supply (0.8 A/W delivered to the plasma).

The impurity-control and particle-exhaust system consists of three high-recycling, toroidal-field divertors (Sections 5, 11, and 17). The TITAN designs take advantage of the beta-limited confinement observed in RFP experiments [12,13] to operate with a highly radiative core plasma, deliberately doped with a trace amount of high- Z Xe impurities (Section 5). The highly radiative plasma distributes the surface heat load uniformly on the first wall (4.6 MW/m^2). Simultaneously, the heat load on the divertor target plates is reduced to less than about 9 MW/m^2 . The ratio of impurity density to electron density in the plasma is about 10^{-4} , Z_{eff} is about 1.7, and 70% of the core plasma energy is radiated (an additional 25% of the plasma energy is radiated in the edge plasma).

The "open" magnetic geometry of the divertors (Section 4.4), together with the intensive radiative cooling, leads to a high-recycling divertor with high density and low temperature near the divertor target ($n_e \simeq 10^{21} \text{ m}^{-3}$, $T_e \simeq 5 \text{ eV}$) relative to the upstream separatrix density and temperature ($n_e \simeq 2 \times 10^{20} \text{ m}^{-3}$, $T_e \simeq 200 \text{ eV}$). The radial temperature profile is calculated to decay sharply to 2 eV near the first wall (Section 5). Negligible neutral-particle leakage from the divertor chamber to the core plasma and adequate particle exhaust are predicted. The first-wall and divertor-plate erosion rate is negligibly small because of the low plasma temperature and high density at that location.

9.2. CONFIGURATION

Detailed subsystem designs for TITAN-I FPC are given in Sections 10 through 14. The parameters of the TITAN-I reference design point, based on detailed subsystem design, are included in Appendix A and follows the DOE/OFE standard reporting format. Appendix A also includes detailed cost tables and parametric systems code predictions of subsystem parameters for comparison with DOE/OFE tables. The elevation view of the FPC is shown in Figures 9.2-1. Figures 9.2-2 and 9.2-3 show the general arrangement of the TITAN-I reactor.

One of the unique features of the TITAN-I design is that the entire FPC operates inside a vacuum tank, made possible because of the small physical size of the reactor (Figure 9.2-1). The vacuum-tank concept moves the vacuum boundary well away from the harsh radiation and thermal environment allowing for a more robust and reliable design. During maintenance of the FPC, the weld at the lid of the vacuum tank must be cut and then re-welded after the maintenance is completed. Although a design with individual vacuum ducts leading to each of the three divertor chambers was considered and is possible, remote cutting and welding of that complex geometry is expected to be much more difficult.

The TITAN-I vacuum tank also provides an additional safety barrier in the event of an off-normal incident. The entire primary-coolant system is enclosed within the containment building, which is filled with argon as a cover gas in order to reduce the probability of a lithium fire in case of major rupture of coolant pipes. Drain tanks are provided below the FPC (Figure 9.2-1) to recover and contain any lithium spilled in the vacuum tank or the reactor building. The drain-tank system connected to the vacuum tank is evacuated during normal operation. The entire primary-coolant system is located above the FPC in order to eliminate the possibility of a complete loss-of-coolant accident (Figures 9.2-1 to 9.2-3).

The TITAN plasma is ohmically heated to ignition by using a set of normal-conducting ohmic-heating (OH) coils and a bipolar flux swing. The TITAN start-up requires minimum on-site energy storage, with the start-up power directly obtained from the power grid (maximum start-up power is 500 MW). An important safety design guideline for TITAN-I allows no water inside the containment building and vacuum vessel, in order to reduce the probability of lithium-water reactions (Section 13). As a result, the OH coils are cooled by helium gas. A pair of relatively low-field superconducting equilibrium-field (EF) coils produce the necessary vertical field and a pair of small, copper EF trim coils provide the exact equilibrium during the start-up and OFCD cycles. The poloidal-field-

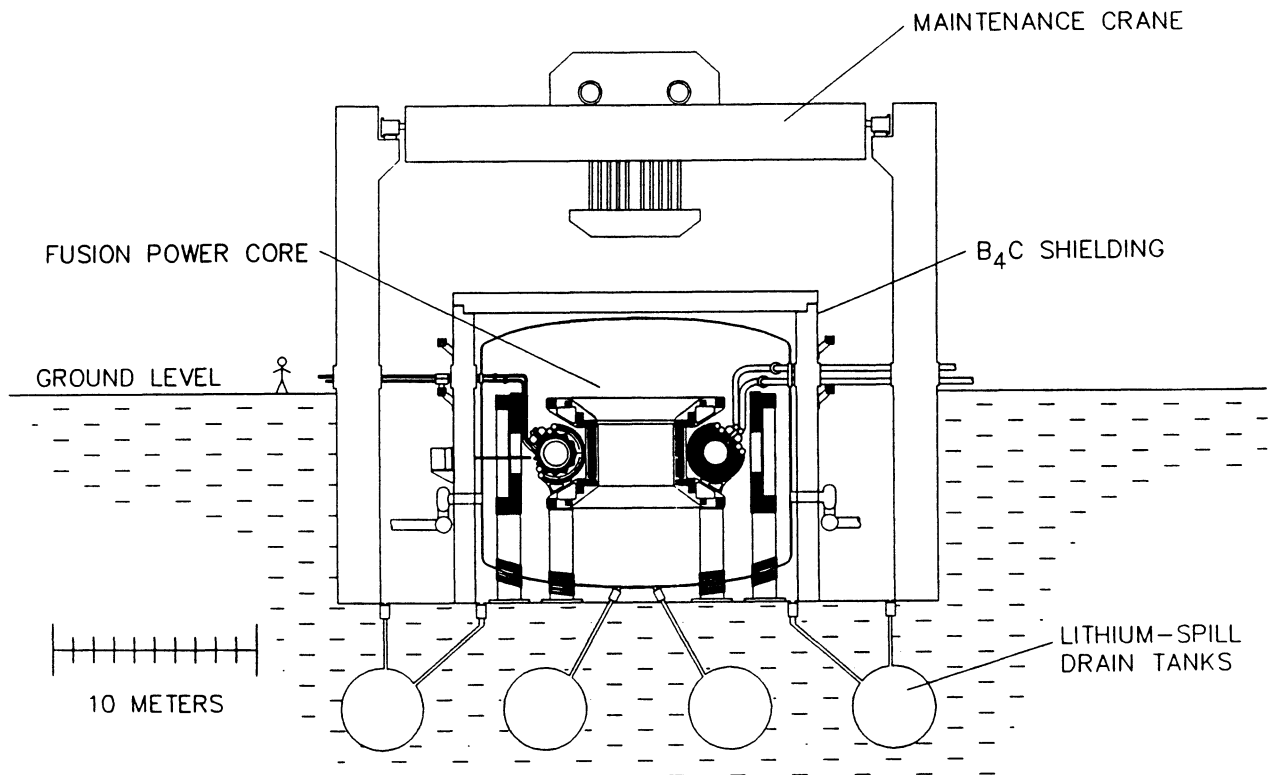


Figure 9.2-1. Elevation view of the TITAN-I reactor building through the reactor centerline showing the reactor vault, the maintenance crane, and the vacuum tank.

coil arrangement allows access to the complete reactor torus by removing only the upper OH-coil set.

Another unique feature of the TITAN-I design is that the divertor and the toroidal-field (TF) coils are based on the integrated-blanket-coil (IBC) concept [14]. The IBC concept utilizes the poloidally flowing lithium coolant of the blanket as the electrical conductor for the divertor and TF coils. Although lithium is about 20 times more resistive than copper, the low toroidal-field requirement of RFPs, combined with the large cross-sectional area available to the IBC, results in acceptable power requirements for TF and divertor coils. The joule heating in the TITAN-I divertor and TF coils are, respectively, 120 and 24 MW. The IBC concept reduces the need to shield the coils significantly, improves neutronics efficiency and energy recovery, reduces the number of components

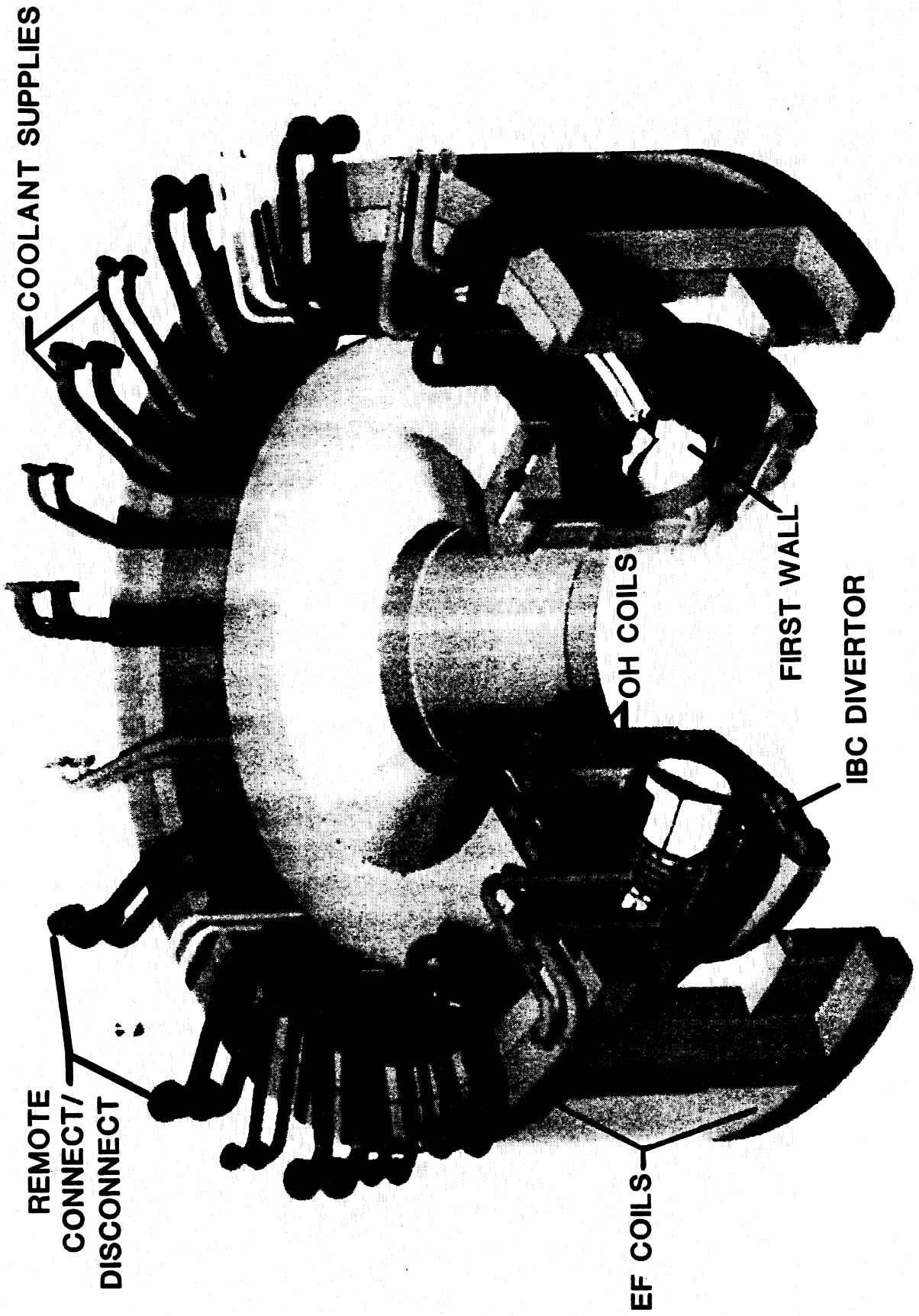


Figure 9.2-2. The TITAN-I fusion power core.



Figure 9.2-3. Cut-away view of the TITAN-I fusion power core.

in the FPC, reduces the toroidal-field ripple, and allows direct access to the blanket and shield assemblies, thereby easing the maintenance procedure.

Poloidal cross sections of the TITAN-I FPC through a divertor module and through a blanket section are shown, respectively, in Figures 9.2-4 and 9.2-5. The geometry, size, and configuration of the first wall, blanket, shield and the associated coolant channels are established primarily by thermal-hydraulic, structural, and neutronics considerations. The dominant magnetic field at the plasma edge (or first wall) in the RFP is poloidal. Since, the TITAN-I FPC is cooled by lithium, the coolant channels in the first wall and blanket are aligned with the poloidal field to minimize the induced MHD pressure drops.

The TITAN reactors operate with a highly radiative core plasma in order to distribute the plasma heat load uniformly on the first wall. Simultaneously, the heat load on the divertor target plates is reduced to manageable levels. As a result, the first wall intercepts the radiation heat flux of about 4.6 MW/m^2 . The TITAN-I first wall is made of a bank of circular tubes. Tubular coolant channels with circular cross sections are suitable for the first wall, since a circular tube has the best heat-transfer capability (highest Nusselt number) and highest strength. In addition, tubes are easy to manufacture with small tolerances in size and wall thickness. To adjust for the shorter toroidal length on the inboard as compared to the outboard, the first-wall tubes slightly overlap on the inboard side of the torus, as is shown in Figure 9.2-6. Consequently, two sets of coolant tubes are used; one set has a slightly larger poloidal diameter than the other. The inside diameter and wall thickness of the first-wall coolant tubes are, respectively, 8 and 1.25 mm. The inside diameter of the first-wall tubes reflects a compromise between the total number of coolant tubes and the heat-transfer coefficient; reducing the diameter increases the number of tubes, which may result in a lower reliability but increases the heat-transfer coefficient. The tube wall thickness of 1.25 mm includes a 0.25-mm allowance for erosion (the first-wall erosion is estimated to be negligible).

The blanket and shield coolant channels are designed with the consideration of heat transfer, blanket energy multiplication, tritium breeding, and shielding requirements. The overall thickness of the blanket and shield is 75 cm. The 28-cm-wide IBC zone is located 1 cm behind the first wall and consists of 6 rows of tubular coolant channels with an inside diameter of 4.75 cm and a wall thickness of 2.5 mm. The primary reason for using tubular coolant channels for the IBC zone, which results in more void, is to reduce the number of load-bearing welded joints (associated with using square ducts) near the plasma. The IBC coolant channels have varying cross sections (Figure 9.2-6) in order to minimize the void fraction of this zone. As a result, the IBC zone consists of 18% structure, 72% lithium, and 10% void by volume.

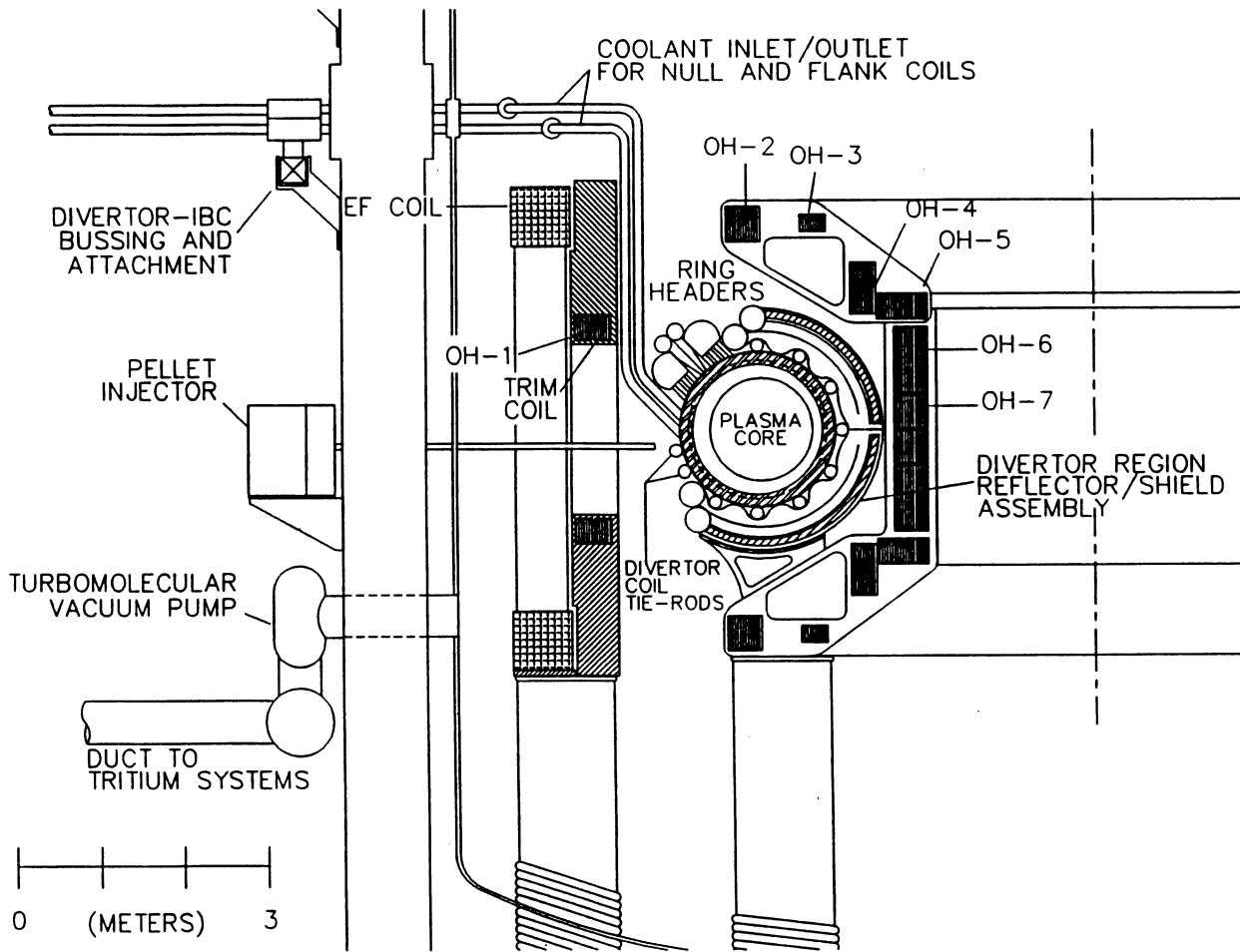


Figure 9.2-4. Poloidal cross section of the TITAN-I FPC through one of the divertor modules.

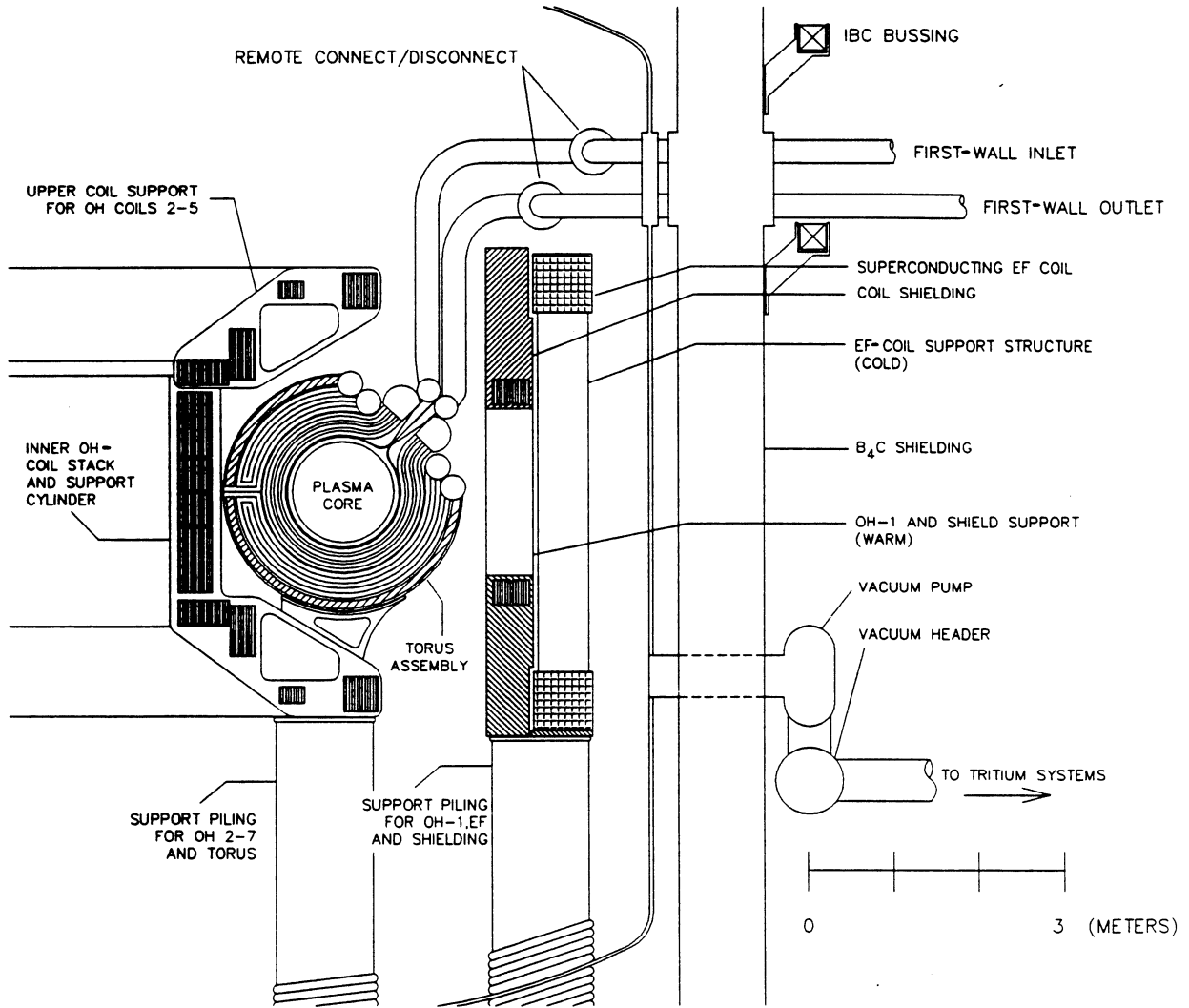


Figure 9.2-5. Poloidal cross section of the TITAN-I first-wall and blanket coolant channels.

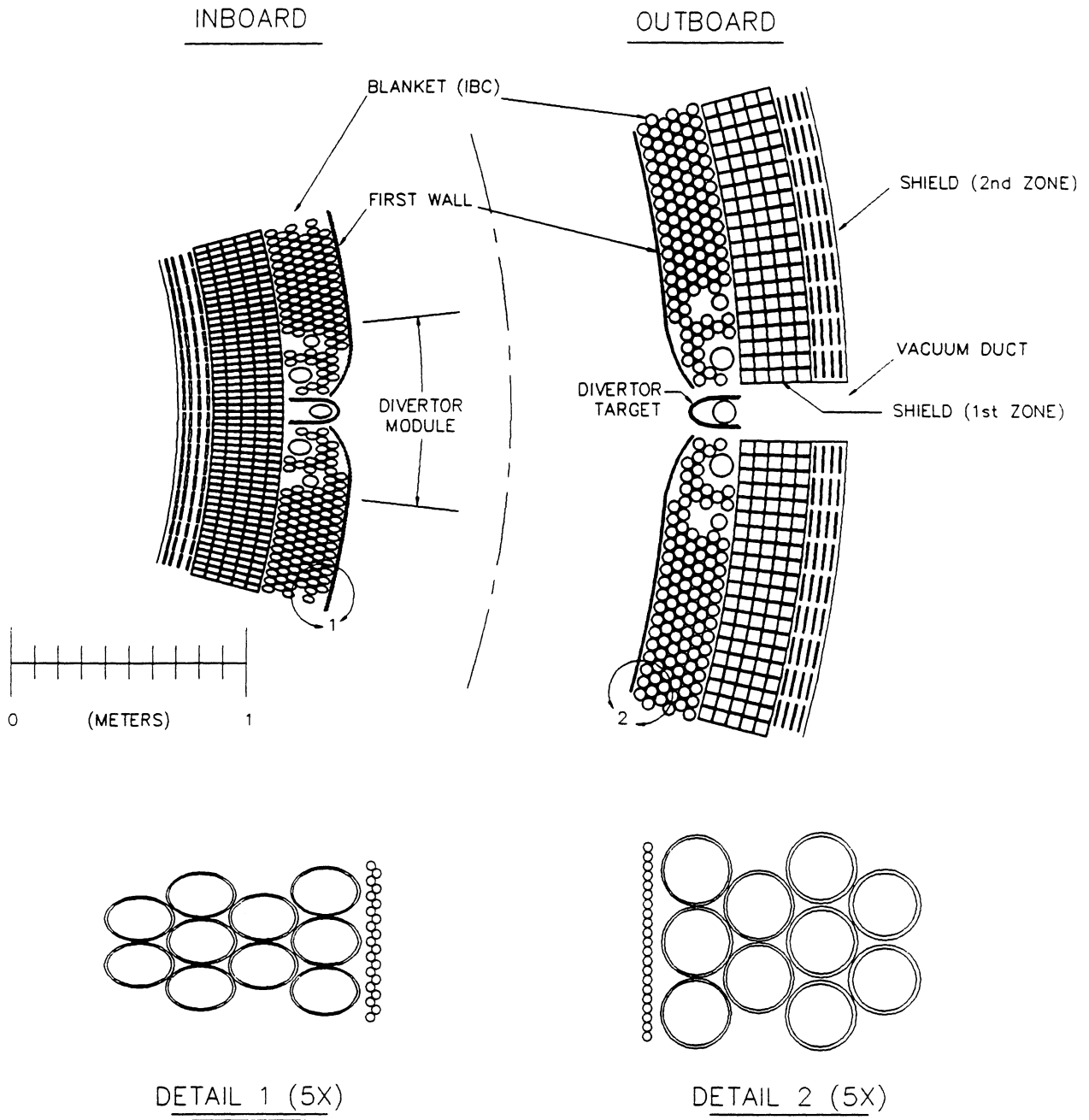


Figure 9.2-6. Horizontal, midplane cross section of the TITAN-I FPC through blanket and divertor regions.

The 45-cm-thick hot shield is located 1 cm behind the IBC and has two zones. The first zone is 30 cm thick and consists of 5 rows of square coolant channels with outer dimensions of 6 cm and a wall thickness of 5 mm. The inside corners are rounded and have a radius-to-wall-thickness ratio of unity. The structure volume fraction is 30%, the coolant volume fraction is 70%, and there is no void. The second zone of the hot shield is 15 cm thick and consists of 4 rows of rectangular channels with thick walls to increase the structure volume fraction in this zone. The structure volume fraction is 90% and the coolant volume fraction is 10%. The channels have outer dimensions of 11.25 cm by 3.75 cm and a wall thickness of 16.25 mm.

The coolant flow in both first wall and blanket are single pass and in the poloidal direction. Double-pass poloidal flow, however, is used in the hot shield. Lithium flows in through the first three square channels of the hot shield, makes a 180° turn at the inboard side, and exits through the last two square channels and the rectangular channels of the hot shield. This double-pass flow pattern allows the hot shield to be constructed of two separate units. During the annual FPC maintenance, the top half of the shield will be removed so that the torus assembly (including the first-wall, IBC, and divertor sections) can be replaced. The estimated lifetime of the shield component is four full power years and, therefore, this portion can be reinstalled after the completion of the annual maintenance.

The lifetime of the TITAN-I reactor torus (including the first wall, blanket, and divertor modules) is estimated to be in the range of 15 to 18 MWy/m² with the more conservative value of 15 MWy/m² requiring the change-out of the reactor torus on a yearly basis for operation at 18 MW/m² of neutron wall loading at 76% availability. The lifetime of the hot shield is estimated to be five years. To reduce the rad-waste, therefore, the TITAN-I hot shield is made of two pieces; the upper hot shield is removed during the maintenance procedures and then reused following replacement of the reactor torus.

9.3. MATERIALS

The advantage of vanadium-base alloys over others for fusion-reactor structural materials has been pointed out in previous publications [15,16]. In particular, when compared with ferritic-steel alloys, vanadium-base alloys exhibit better physical, mechanical, and nuclear properties. For example, compared to HT-9, vanadium-base alloys have a higher melting temperature, a lower thermal expansion coefficient, and a lower density. Furthermore, compared to ferritic alloys at 1 MW/m² of neutron wall load, vanadium-base

alloys have about one-half the nuclear-heating rate ($\sim 25 \text{ W/cm}^3$), about a third of the helium-generation rate ($\sim 57 \text{ He-appm/y}$), about half the hydrogen-production rate ($\sim 240 \text{ H-appm/y}$), and lower long-term afterheat [15].

The high melting temperature of vanadium alloys ($T_m = 1890^\circ\text{C}$) has significant bearing on safety related issues. The higher ultimate tensile strength ($\sigma_u \sim 600 \text{ MPa}$ at 600°C), the lower expansion coefficient, and the slightly higher thermal conductivity of vanadium-base alloys are reflected in higher thermal stress factors when compared to HT-9 [15]. The thermal stress factor is a measure of heat load capability. The high T_m coupled with a high thermal stress factor, promises high operating-temperature and high neutron-wall-loading capabilities. High T_m combined with a low helium-production rate is also desirable for fusion reactor materials, since below $\sim 0.5T_m$ (in K), strength and ductility are retained and fracture remains transgranular [17] ($0.5 T_m$: vanadium $\simeq 1082 \text{ K}$, HT-9 $\simeq 846 \text{ K}$). Because helium embrittlement is directly related to the helium production rate, a low helium generation rate in vanadium-base alloys is a very favorable characteristic.

From the three candidate vanadium-base alloys, V-3Ti-1Si is chosen as the primary structural material for TITAN-I, primarily because of its irradiation behavior. It outperforms V-15Cr-5Ti and VANSTAR considering helium embrittlement, irradiation hardening, and swelling after exposure to a damage dose of 40 dpa by fast neutrons. However, V-3Ti-1Si has the lowest thermal-creep resistance of the three alloys (Section 10.2.1).

The effects of gaseous transmutations (*i.e.*, hydrogen and helium) on the mechanical properties of vanadium-base alloys were considered. Based on extrapolation of the limited available data to TITAN-I operating conditions, irradiation hardening and helium and hydrogen embrittlement of V-3Ti-1Si set an upper lifetime limit of approximately 18 MWy/m^2 for the TITAN-I first wall. Irradiation-induced swelling of the V-3Ti-1Si alloy was also investigated and it was concluded that swelling would be negligible for the lifetime of the TITAN-I first wall (Section 10.2.1).

The modified-minimum-commitment method (MMCM) [18] was used to extrapolate the creep-rupture data and to establish the creep behavior during normal and off-normal operating conditions (Figure 9.3-1). From the limited creep data, it appears that V-3Ti-1Si will be able to operate satisfactorily at elevated temperatures (700°C). To include the effects of the irradiation hardening, helium-embrittlement data were used to estimate the maximum allowable design stress based on a $2/3$ creep-rupture-stress criterion (Section 10.2.1). Further creep-rupture experiments are needed to develop more precise creep-rupture models for V-3Ti-1Si.

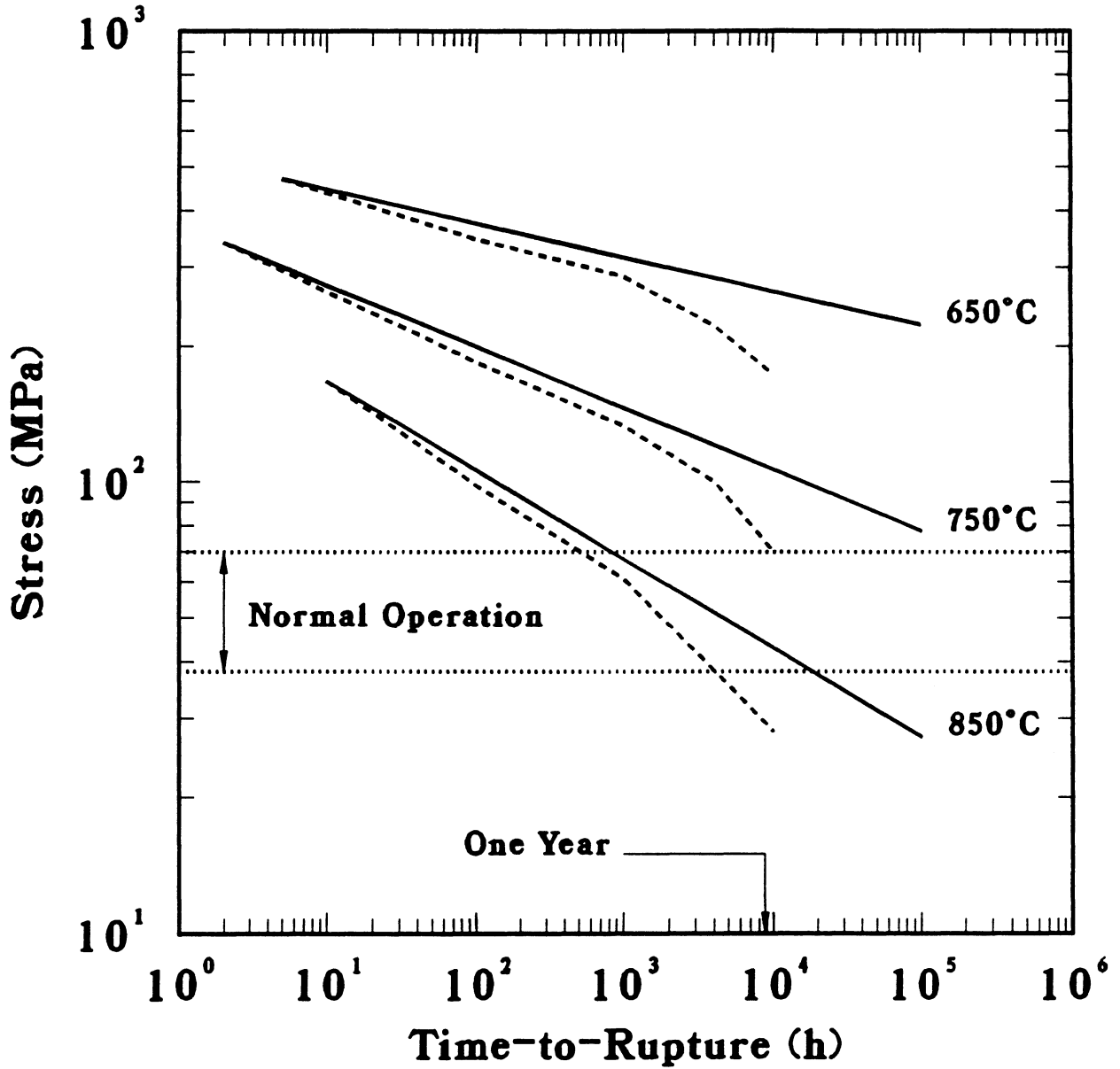


Figure 9.3-1. Creep-rupture stress curves for V-3Ti-1Si at various temperatures estimated by MMCM. Solid lines represent the creep behavior of unirradiated and dashed lines that of irradiated V-3Ti-1Si alloy. Also shown is the expected stress range during the normal operation of the TITAN-I design.

Compatibility of the vanadium-base alloys with lithium coolant was investigated. Recent test results were used to establish the anticipated degree of lithium attack on the V-3Ti-1Si alloy. Various lithium-attack processes were examined with particular attention given to the interaction between vanadium and nonmetallic impurities such as oxygen, nitrogen, carbon, and hydrogen. The limited available data does indicate the possibility of a self-limiting corrosion rate on V-3Ti-1Si because of the formation of complex vanadium-titanium-nitride surface layers (Section 10.2.2). The effects of a bimetallic loop containing liquid lithium were also investigated. Low-carbon, titanium-stabilized ferritic steel exhibits good resistance against lithium corrosion (Section 10.2.2).

In the TITAN-I design, the liquid-lithium coolant flows at a high velocity of 21 m/s in the first-wall channels. The effects of velocity on corrosion rate are complex and depend on the characteristics of the metal and the environment. Velocity affects corrosion by two distinct mechanisms: agitation of reaction constituents can increase reaction rates; and increasing momentum of fluid particles can lead to an increase in wear (*i.e.*, erosion). Increased reaction rates are generally found in aqueous solutions, where the concentration of cations and anions play a large role in corrosion rates. In general, liquid metals do not interact chemically with solid surfaces, therefore, the effects of velocity on corrosion rates of vanadium alloys in a liquid-lithium environment fall mostly into the second category.

Wear by erosion can be caused by intense pressure or shock waves traveling in the fluid. A literature search regarding erosion by liquid lithium showed that this issue has not been investigated in any detail, specifically for vanadium alloys. Most of the research regarding erosion deals with water-steel systems, and particularly distinguishes between particle-free or particle-containing water or slurry. The effects of high-velocity lithium on erosion was estimated using water-steel data. From a very limited set of data on erosion of refractory metals by high-velocity liquid lithium and from the water-steel experience, it seems that lithium velocity of 20 to 25 m/s should not introduce unacceptable erosion rates (Section 10.2.2).

In TITAN-I reactor, electrically insulating materials are not used in direct contact with coolant; therefore coolant compatibility is not a major issue in selecting an insulating material. The selection criteria is based primarily on satisfying minimum irradiation-induced swelling, retention of strength, and minimum radiation-induced conductivity. Organic insulating materials generally do not meet high temperature requirements and suffer from rapid degradation of electrical resistivity when exposed to ionizing radiation. Ceramic insulating materials, on the other hand, possess high melting or decomposition temperatures ($> 2000^{\circ}\text{C}$).

Spinel (MgAl_2O_4) has been chosen as the primary electrical insulating material for

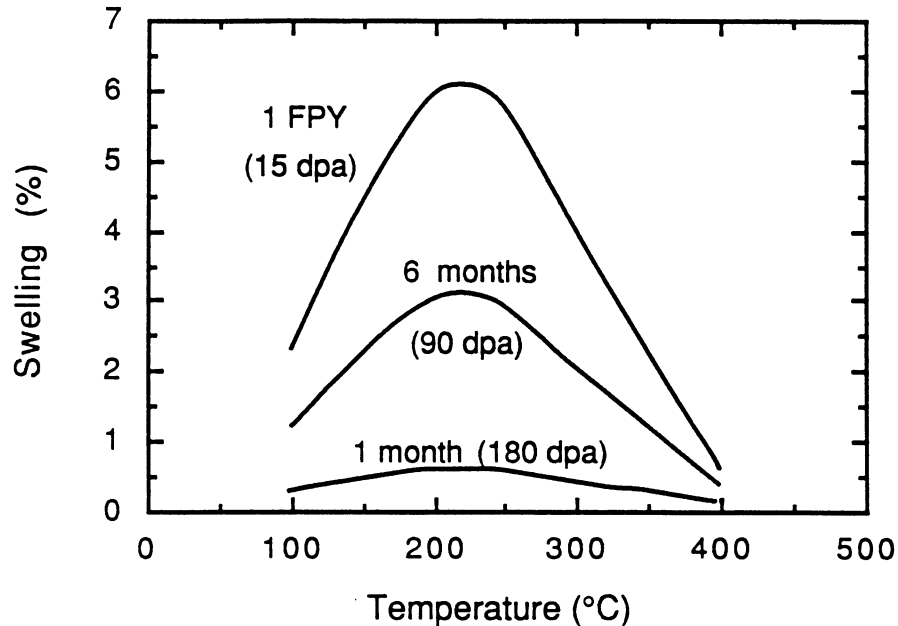


Figure 9.3-2. Swelling of spinel as a function of dpa (or exposure time under 18 MW/m^2 of neutron wall loading) and temperature.

the TITAN-I design, based on excellent resistance to radiation-induced swelling and retention (or increase) of strength (Section 10.2.3). A phenomenological swelling equation was developed as a function of temperature and damage dose. Figure 9.3-2 shows the estimated swelling of spinel at the first wall or divertor of TITAN-I as a function of temperature and exposure time at 18 MW/m^2 of neutron wall load. This swelling curve shows that operating spinel below 150°C or above 300°C ensures low swelling rates ($< 5\%$). High operating temperatures may ensure a low swelling rate but could bring about dielectric breakdown of the insulator. Low-temperature operation ($< 150^\circ\text{C}$) is, therefore, suggested (Section 10.2.3).

9.4. NEUTRONICS

The neutronics design of the blanket and shield for the TITAN reactors is unique because of the high neutron wall loading (18 MW/m^2). The other unique aspect of the TITAN reactors is the use of normal-conducting coils in the toroidal-field, divertor, and

ohmic-heating (OH) magnets. The neutron-fluence limit of the TITAN-I OH magnets is set by the spinel-insulator lifetime and is 3 to 4 orders of magnitude larger than that of a superconductor magnet (1×10^{23} n/m²) [19]. The use of normal-conducting coils with ceramic insulators implies a 0.6 to 0.8 m reduction in the shielding space, and helps maintain the compactness of the FPC design.

Tritium breeding, blanket energy multiplication, afterheat, radiation damage to the structural materials and the OH magnets, annual replacement mass (and cost) of blanket and shield, and the waste-disposal ratings are some of the important parameters that were considered for the neutronics optimization of the TITAN-I design. Neutronics calculations were performed to investigate each of the above parameters based on a 1-D blanket and shield model in a cylindrical geometry, with the center of the poloidal cross section of the plasma located on the centerline of the cylinder. The neutron and gamma-ray transport code, ANISN [20], is used with the cross-section library ENDF/B-V-based MATXS5 processed with the NJOY system at Los Alamos National Laboratory [21].

Scoping calculations were performed for several combinations of blanket and shield thickness with varying amount of structure and different levels of ⁶Li enrichment in the lithium coolant (Section 10.3). It was found that:

1. Most of blankets considered achieved an adequate tritium-breeding ratio (TBR > 1.2 from 1-D full-coverage calculations). Enrichment level of ⁶Li can be used to control the TBR.
2. Manganese stainless-steel shield can increase the blanket energy-multiplication ratio but would impose a potential safety problem because of higher levels of decay afterheat.
3. The energy-multiplication ratio for blankets with a vanadium shield ranges from 1.1 to 1.2. Afterheat levels, however, are considerably lower than those with a manganese shield.
4. A highly enriched ⁶Li coolant (75%) reduces the afterheat level by a factor of ~ 8 for about one hour after shutdown.
5. The atomic displacement in the shield and magnets decreases dramatically as the ⁶Li enrichment increases which reduces the annual replacement mass.

The neutronics scoping studies resulted in the reference blanket and shield design of the TITAN-I illustrated in Figure 9.4-1. The neutronics performance of the reference

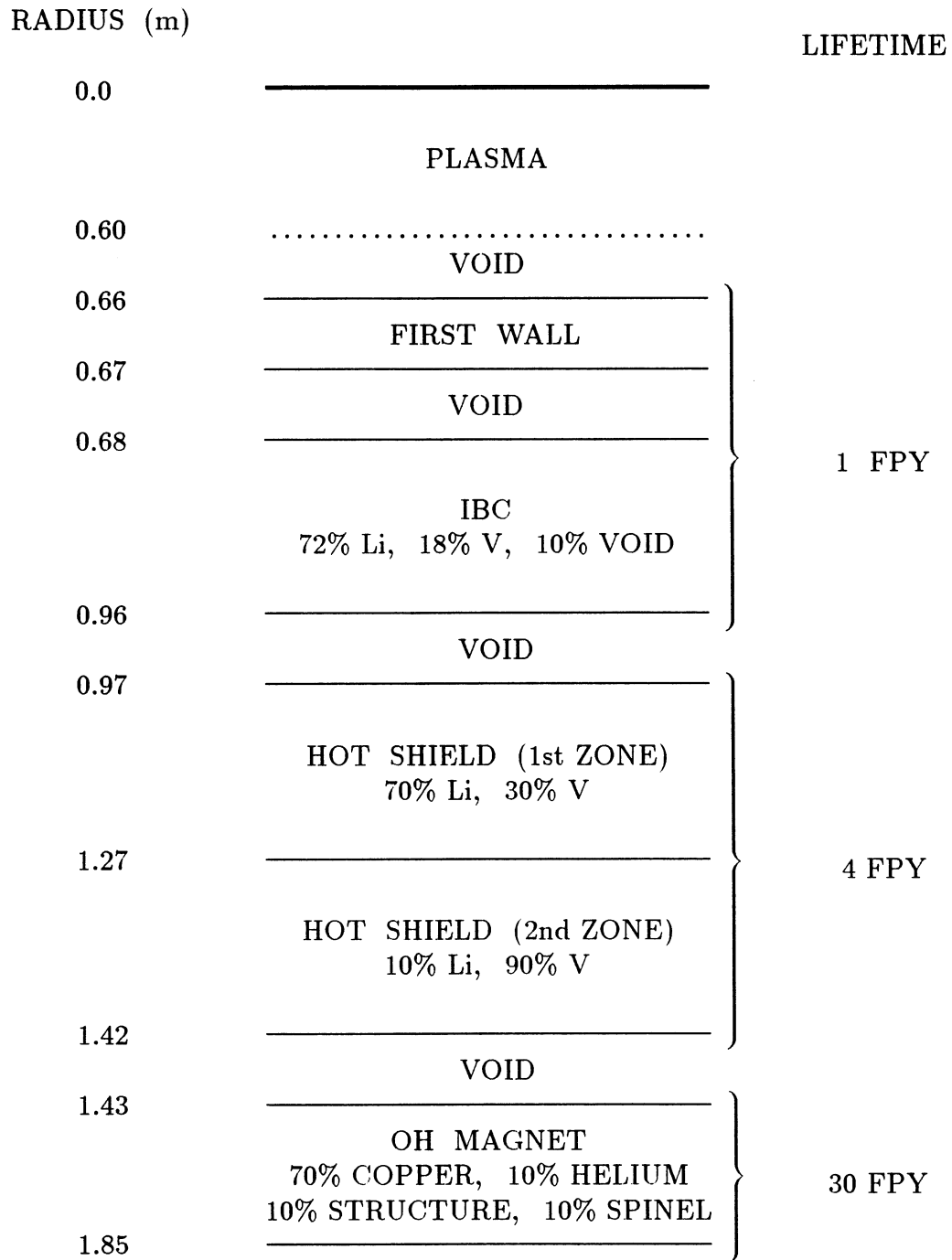


Figure 9.4-1. Schematic of the blanket and shield for the TITAN-I reference design.

Table 9.4-I.
NUCLEAR PERFORMANCE
OF THE TITAN-I REFERENCE DESIGN^(a)

• ⁶ Li enrichment		30%	
• Tritium-breeding ratio:			
⁶ Li (n,α)		1.084	
⁷ Li (n,n',α)		0.247	
TOTAL		1.33	
• Blanket energy multiplication, <i>M</i>		1.14	
• Nuclear heating (MeV per DT neutron):			
	<u>Neutron</u>	<u>Gamma Ray</u>	<u>Sum</u>
First wall	0.341	0.183	0.524
Blanket	7.382	2.603	9.985
Shield (1st zone)	3.148	1.595	4.743
Shield (2nd zone)	0.235	0.560	0.795
TOTAL	11.106	4.941	16.047
OH coils	0.038	0.438	0.476

(a) From 1-D ANISN calculations.

design with a vanadium-alloy shield is given in Table 9.4-I. The tritium-breeding ratio is 1.33 and the total nuclear heating is 16.05 MeV per DT neutron resulting in a blanket energy multiplication of 1.14. The maximum fast-neutron fluence at the OH magnet after 30 full-power years (FPY) of operation at 18 MW/m² of neutron wall loading is found to be 7×10^{26} n/m², and is substantially lower than the estimated lifetime limit of 2×10^{27} n/m² for the spinel insulator.

The ⁶Li enrichment of 30% was selected for the reference design because of the improved afterheat and magnet protection performance and the acceptable enrichment cost. Future optimization of the TITAN-I design may be possible by considering different low-activation reflector materials to reduce cost and by performing very detailed trade-off studies between ⁶Li enrichment, cost, annual-replacement-mass, and waste-disposal issues.

The final design parameters were verified by a set of 3-D neutronics calculations with the Monte Carlo code, MCNP [22], taking into account the toroidal geometry and the divertor modules. Non-IBC blanket tubes are incorporated in the space around the divertor and target plates. The hot-shield is extended behind the divertor coils except that a 90° opening in the poloidal direction is provided on the outboard divertor region for pumping (Figure 9.2-6). The tritium-breeding ratio for the 3-D model of the reference design is 1.18 and the maximum fast-neutron fluence at the OH magnet in the inboard region is 1.6×10^{27} n/m², which is well below the assumed lifetime limit for the spinel insulator.

9.5. THERMAL AND STRUCTURAL DESIGN

The TITAN-I FPC is cooled by liquid lithium. One of the issues for liquid-metal coolants in fusion reactors is the MHD-induced pressure drop. In an RFP fusion reactor such as TITAN, the toroidal magnetic field at the first wall is small; thus the MHD pressure drop can be kept low by alignment of the coolant channels primarily in the poloidal direction.

The TITAN designs operate with a highly radiative core plasma, in order to distribute the surface heat load uniformly on the first wall (4.6 MW/m²) and to keep the heat load on the divertor target plates at a manageable level. Cooling of the high-heat-flux components, such as the first wall and divertor target plates, represents one of the critical engineering aspects of compact fusion reactors. The use of a highly radiative core plasma

and the resulting distribution of the heat fluxes over the first wall is central to the solution to this problem. The main thermal-hydraulic design features of the TITAN-I FPC are:

1. First-wall sputtering is almost negligible as a result of the operation with a high-recycling divertor.
2. Small-diameter, thin-walled, circular coolant tubes are used for the first wall.
3. First-wall and blanket coolant circuits are separated.
4. Coolant channels are aligned with the dominant, poloidal magnetic field.
5. Turbulent-flow heat transfer is used to remove the high heat flux on the first wall.

For a given size for the first-wall coolant tubes, the maximum wall-temperature constraint would result in a maximum limit on the surface heat flux. Turbulent coolant flow, which is accompanied by a higher Nusselt number (Nu), allows a higher surface heat flux compared with laminar coolant flow. The magnetic field, generally, tends to suppress turbulence in the flow of an electrically conducting fluid, and the onset of turbulence would occur at higher Reynolds numbers compared with non-MHD pipe flow.

A few studies on the turbulent heat transfer in liquid metals in the presence of a magnetic field [23-25] are available. Kovner *et al.* [23] performed experiments on the effect of a longitudinal magnetic field on turbulent heat transfer in liquid-galium flow in a tube. The following empirical correlation for Nusselt number was then proposed:

$$Nu = 6.5 + \frac{0.005Pe}{1 + 1890(Ha_{\parallel}/Re)^{1.7}}, \quad (9.5-1)$$

where Re is the Reynolds number, Ha_{\parallel} is the parallel Hartmann number, $Pe = Re Pr$ is the Peclet number, and Pr is the Prandtl number. Even though Equation 9.5-1 is based on experimental data up to $Ha_{\parallel} = 550$, it is expected to hold beyond this range. Other experimental data and numerical studies show similar dependence [24,25]. Figure 9.5-1 shows the variation of the Nusselt number with Peclet number for $B = 0$, $Ha_{\parallel} = 1000$, and $Ha_{\parallel} = 3040$ (the expected Ha_{\parallel} in the TITAN-I first wall). The range of the experimental data is also shown in this figure.

The nonuniform circumferential heat flux on the first-wall coolant tubes will reduce the turbulent Nusselt number at the point of higher heat flux, as is shown for the case of laminar flow (Section 10.4.3). For the TITAN-I design, the Nu given by Equation 9.5-1 is reduced by a factor of two to account for this nonuniform circumferential heat flux until

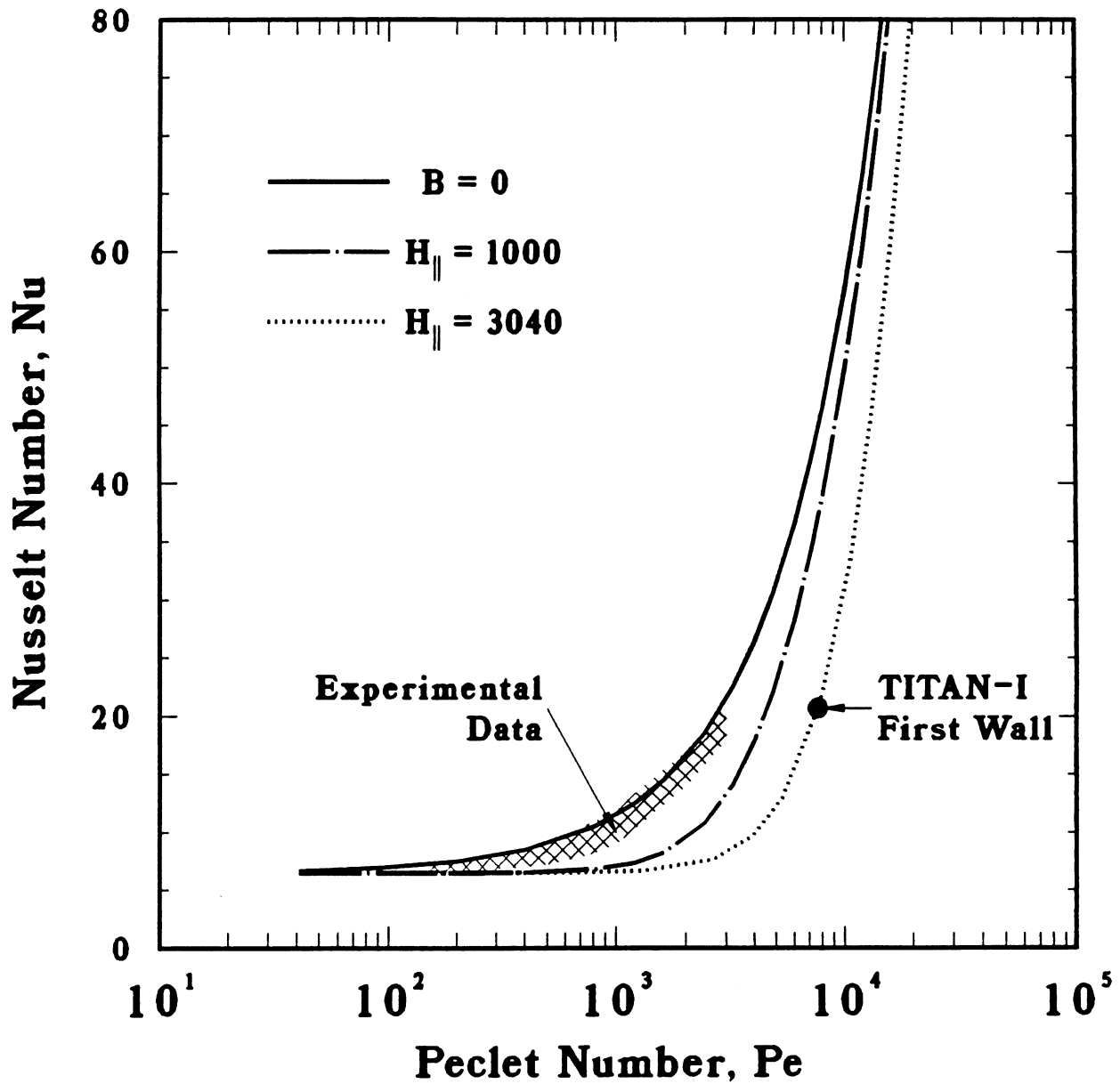


Figure 9.5-1. Variation of the Nusselt number, Nu , with the Peclet number, Pe for turbulent flow as predicted by Equation 9.5-1. The range of experimental data as well as the operating point of the TITAN-I first wall are also shown. The Nusselt number from this graph should be halved to account for nonuniform heat flux on the TITAN-I first wall.

further data becomes available. The MHD pressure drops were calculated by various correlations appropriate for TITAN-I design (Section 10.4).

In order to complete the thermal-hydraulic design, pressure and thermal stresses in the FPC coolant channels were estimated by 1-D equations (along r , radial direction in the tube) for a thick-walled tube. Two-dimensional thermomechanical analyses of the TITAN-I FPC were also performed using the finite-element code, ANSYS [26], which verified the 1-D analysis (Section 10.4.6).

A thermal-hydraulic design window for compact, liquid-lithium-cooled RFP reactors was found based on certain design constraints such as the maximum allowable temperature of the structure (750°C), the maximum allowable pressure and thermal stresses in the structure (respectively, 108 and 300 MPa), and the maximum allowed pumping power (5% of plant output). The maximum allowable temperature of the structure corresponds to a maximum value for the average coolant exit temperature for a given heat flux. The maximum allowable stress and the maximum allowed pumping power would result in minimum values for the average exit temperature of the coolant. The design window for the coolant exit temperature is then located between these limits. Other parameters impacting the design window are the neutron wall loading, the coolant channel size, and the coolant inlet temperature.

Figure 9.5-2 illustrates the thermal-hydraulic design window for the TITAN-I first wall and shows that a design with a radiation heat flux on the first wall of 4.9 MW/m^2 is possible (corresponding to 20 MW/m^2 of neutron wall load at 95% total radiation fraction). The sudden change in the slope of the top curve in Figure 9.5-2 is caused by the change from laminar to turbulent flow. The flow in blanket and shield is always laminar. The total pumping-power limit of 5% of electric output is more restrictive than the pressure stress of 108 MPa. The thermal-stress limit is not reached up to the maximum heat flux on the first wall.

The main results of the thermal-hydraulic analysis of the TITAN-I first wall are given in Table 9.5-I. The coolant flow velocity in the TITAN-I first-wall tube is 21 m/s and the maximum pressure drop is 10 MPa. The coolant velocities in the 1st and 6th (last) rows of the IBC coolant channels are, respectively, 0.5 and 0.2 m/s. The pressure drops in the 1st and 6th rows are 3.0 and 0.5 MPa, respectively. The maximum pressure drop in the divertor coolant circuit is 12 MPa. In order to simplify the design, the first-wall and divertor coolants are supplied from the same circuit with a delivery pressure of 12 MPa. One single orifice is used to reduce the lithium pressure to 10 MPa for the first-wall circuit. Additional orifices are used, wherever necessary, in order to reduce the coolant pressure from 12 MPa to the required inlet pressure of the individual rows of divertor coolant

Table 9.5-I.

THERMAL-HYDRAULIC DESIGN OF TITAN-I FIRST WALL

Pipe outer diameter, b	10.5	mm
Pipe inner diameter, a	8.0	mm
Wall thickness, t	1.25	mm
Erosion allowance	0.25	mm
Structure volume fraction	0.400	
Coolant volume fraction	0.375	
Void volume fraction	0.225	
Coolant inlet temperature, T_{in}	320	°C
Coolant exit temperature, $T_{ex,FW}$	440	°C
Maximum wall temperature, $T_{w,Max}$	747	°C
Maximum primary stress	50	MPa
Maximum secondary stress	288	MPa
Coolant flow velocity, U	21.6	m/s
Pressure drop, Δp	10	MPa
Total pumping power ^(a)	37.7	MW
Reynold's number, Re	1.90×10^5	
Magnetic Reynold's number, Re_m	0.48	
Parallel Hartmann number, H_{\parallel}	3.04×10^3	
Perpendicular Hartmann number, H_{\perp}	2.01×10^2	
Parallel magnetic interaction parameter, N_{\parallel}	48.6	
Perpendicular magnetic interaction parameter, N_{\perp}	0.21	
Nusselt number, Nu	10.35	
Prandtl number, Pr	4.08×10^{-2}	
Peclét number, Pe	7.76×10^3	

(a) A pump efficiency of 90% is assumed.

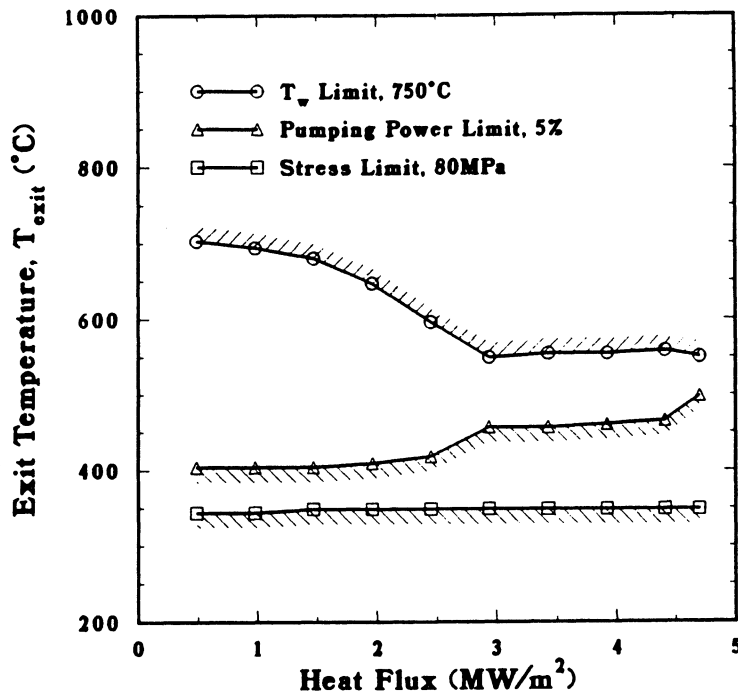


Figure 9.5-2. The thermal-hydraulic design window for the TITAN-I FPC.

tubes. The supply pressure of the blanket coolant pump is 3 MPa. Orifices are used to reduce the pressure to the required values at the inlet of each row of IBC channels.

9.6. MAGNET ENGINEERING

Three types of magnets are used in the TITAN-I design (Figure 9.2-4). The ohmic-heating (OH) and the equilibrium-field (EF) trim coils are normal-conducting with copper alloy as the conductor, spinel as the insulator, and gaseous helium as the coolant. The main EF coils are made of NbTi conductor and steel structural material. These poloidal-field (PF) coils are designed to last the life of the plant. Because of their simple geometry, the robust support structure, and the relatively low field produced by these coils, little or no extrapolation of current technology should be required.

The divertor and the toroidal-field (TF) coils of the TITAN-I design are based on the integrated-blanket-coil (IBC) concept [14]. The IBC as applied to TITAN-I also acts as the toroidal-field driver coil for the oscillating-field current-drive system, OFCD (Section 7). The toroidal-field (TF) coils of TITAN-I oscillate at 25 Hz with currents ranging between 30% to 170% of the mean steady-state value of 7.0 MA-turns (including

the currents in the divertor trim coils). The PF coils also oscillate at 25 Hz. It is also necessary to oscillate the divertor coils to maintain the plasma separatrix at the proper location.

The IBC design encounters several critical engineering issues: (1) steady-state and oscillating power-supply requirements for low-voltage, high-current coils; (2) time-varying forces caused by the OFCD cycles; (3) integration of the primary heat-transport system with the electrical systems; (4) sufficient insulation to stand off induced voltages; and (5) suitable time constants for various components to permit the coil currents to oscillate at 25 Hz. Heat removal is not an issue for IBC because the joule heating is produced directly in the primary coolant.

Design of the power supplies is one of the critical issues for IBC. The low number of electrical turns available (12 for the TITAN-I design) results in low-voltage, high-current coils (3.85 V, 520 kA per coil). Power supplies rated for such conditions would be expensive and would exhibit high internal-power losses if based on technology that is currently available. Connecting all 12 IBCs of TITAN-I in series would raise the voltage of the power supply to a more manageable value. However, the IBC approach requires that the electrical and hydraulic systems be physically connected, and that the intermediate heat exchangers (IHxs) and coolant pumps should be grounded (*i.e.* no electric current flowing through the IHxs and pumps).

Figure 9.6-1 illustrates the electrical and hydraulic layout of the TITAN-I IBC system. The TITAN-I FPC comprises three sectors which are connected to each other through the divertor modules. To increase the power-supply voltage, the four IBCs in each sector are electrically connected in series in the TITAN-I design and allow a better match of current and voltage for the power supply (15.4 V, 541 kA). This circuit, however, requires two IHxs per sector for the IBC cooling circuit. Figure 9.6-1 shows that, because of the series connection of the IBCs and grounding of the pumps and heat exchangers, a leakage current will flow through the cold and hot legs. The leakage current is small in magnitude but causes unequal coil currents, necessitating a small balancing power supply to accompany each main power supply, as is indicated in Figure 9.6-1. The load on each balancing power supply (7.7 V and 27 kA) is much smaller than that of the main power supply (15.4 V and 541 kA) and leaks through the cold legs to ground.

The impurity-control system of the TITAN-I design consists of three toroidal-field divertors. Each divertor consists of one nulling coil and two flanking coils to produce the local effects necessary for field nulling. Because of the loss of coverage of TF IBCs in the divertor region, a pair of trim coils is added to each divertor in order to localize the toroidal-field ripple. The divertor IBCs operate at relatively higher current densities

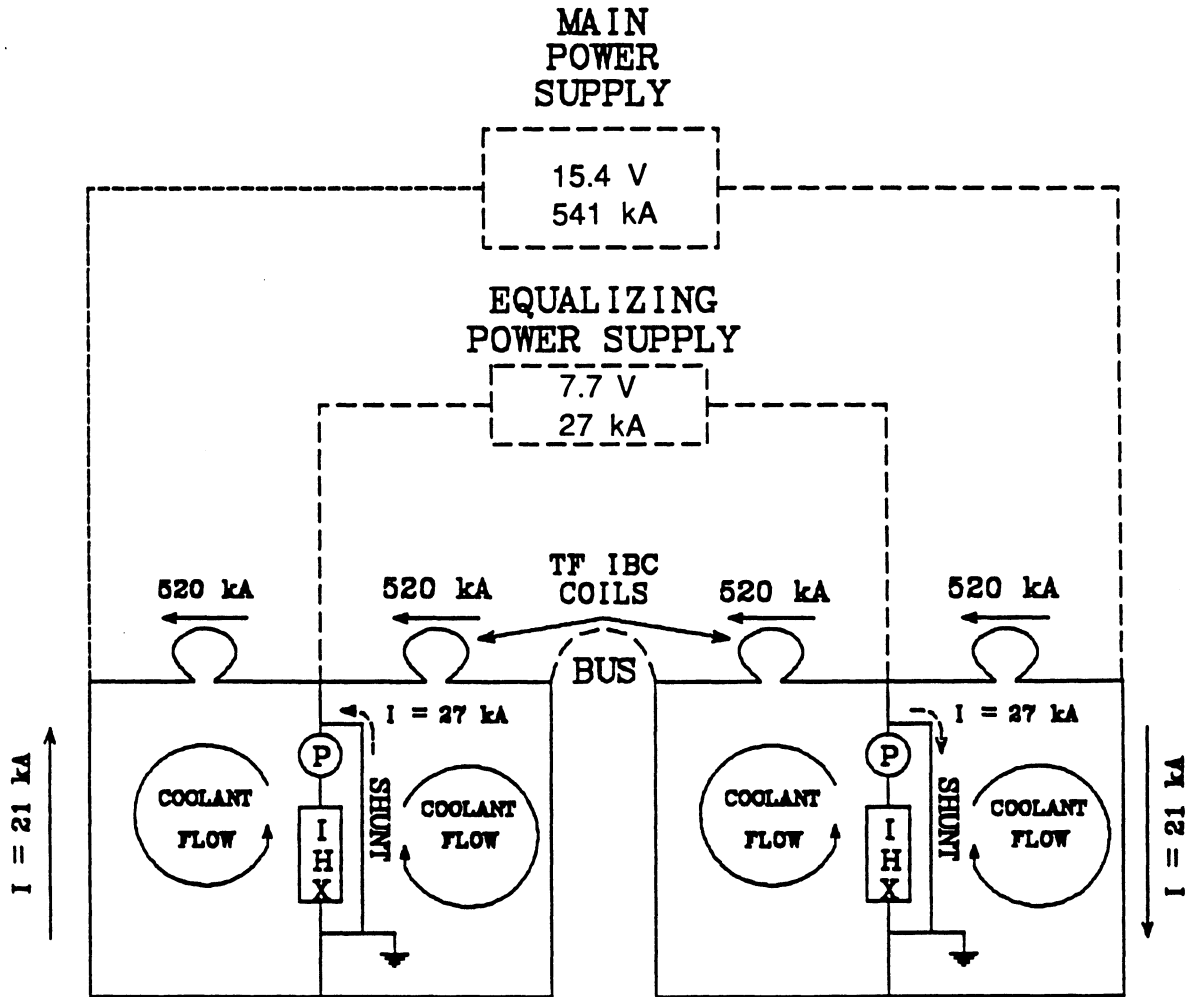


Figure 9.6-1. Schematic of the electrical and hydraulic layout of TITAN-I TF IBCs.

than the TF coils, thereby requiring much greater voltages. Furthermore, the current in each nulling coil is exactly equal to that of the two flanking coils. The divertor IBCs are connected in order to take advantage of the symmetric currents and larger voltages. Because equalizing power supplies are not needed for the divertor IBCs, only two power supplies per divertor module are required. The joule losses in the divertor IBCs (three divertors) are 117 MW with additional 3.5-MW losses in the hot legs.

Because of the large impedance of the toroidal-field circuit during the OFCD cycles (about $0.1 \text{ m}\Omega$ for each TF coil), the oscillating voltage on each TF coil ($\sim 50 \text{ V}$) is much larger than the steady-state value ($\sim 3.8 \text{ V}$). Detailed analyses of the OFCD power supplies and the leakage currents were not performed because the results are sensitive to the impedances of the hot and cold legs which in turn depend on the piping arrangement. Instead, the leakage currents were calculated based on simple estimates of the internal inductances of coolant pipings. The joule losses in the TF coils during the OFCD cycle are estimated to be 25.6 MW for the steady-state portion (24 MW in the coil and 1.6 MW in the hot and cold legs) and 16 MW for the oscillating voltages (15 MW in the coils and 1 MW in the hot and cold legs).

It is necessary to oscillate the divertor coils during the OFCD cycle to maintain the plasma separatrix at the proper location. Since the magnitude of oscillation of the toroidal flux was found to be small, the strength of the toroidal field on the plasma surface would be directly proportional to the reversal parameter and the magnitude of the current oscillations in the divertor coils would be about $2/3$ of the steady-state value. The voltage oscillations applied to the divertor coils are roughly equal to the steady-state values, in contrast to the TF coils, because the divertor coils operate at much higher current densities and have higher resistances. The oscillating losses in the divertor IBCs are estimated at 26 MW in the coils and 0.8 MW in the hot and cold legs.

Interaction of the current in the IBC with the reactor magnetic fields produces forces on the TF and divertor coils. These forces are much lower than the corresponding forces in tokamaks since the coil currents are much lower in RFPs. The magnitudes of the forces on the TITAN-I IBCs vary over time as the currents oscillate during the OFCD cycle. Hence, structural supports are designed for the peak loads (Section 10.5.3). Dynamic structural analysis also shows that failure will not occur as a result of these cyclic forces.

9.7. POWER CYCLE

One of the advantages of using liquid lithium as the coolant for TITAN-I is the ability to remove the thermal energy from the reactor at a high thermal potential so that a high power-cycle efficiency can be realized. An important feature of the thermal-hydraulic design of the TITAN-I first wall and blanket is the separation of the coolant circuits for these components in order to handle the high surface-heat flux on the first wall. As a result, the first-wall coolant has a much lower exit temperature (440 °C) than the blanket and shield coolant (700 °C). The divertor coolant also has a different exit temperature (540 °C). The inlet temperatures to all three circuits are kept the same primarily for simplicity. Since the thermal power in the divertor circuit is very small (1% of total thermal power), the first-wall and divertor coolants are mixed at exit, leading to two separate streams of the primary coolant which remove, respectively, 765 and 2170 MWt of power with exit temperatures of 442 and 700 °C.

The TITAN-I reference design uses two separate power cycles: one for the first-wall and divertor stream and the other for the IBC and shield stream (Section 10.6.2). Each of these two power cycles has a separate IHX, steam generators, and turbine-generator set. The TITAN-I FPC consists of three toroidal sectors. One IHX and one steam generator are required per sector for the first-wall and divertor coolant stream. The steam produced in these three steam generators is mixed and fed to a single turbine-generator set. For the IBC and shield stream, two IHXs are used per sector, based on electrical engineering requirements of the IBCs. The secondary coolants of each pair of these heat exchangers are mixed and fed to one steam generator (per sector). As in the first-wall and divertor cycle, the steam from all three steam generators is mixed and fed to a single turbine-generator set.

The power cycle analysis is performed by the computer code PRESTO [27]. The pinch-point temperature difference in the steam generators of each of these power cycles is kept above 20 °C. For both the first-wall and divertor cycle and the IBC and shield cycle, the temperature loss in the IHXs is set at 20 °C. The first-wall and divertor power cycle is a superheat Rankine cycle with four stages of feed-water heating. Reheat of the steam after expansion through the high-pressure turbine is not used. The total thermal power in the first-wall and divertor power cycle is 765 MWt and the gross thermal efficiency is 37.0%. The IBC and shield power cycle is a superheat Rankine cycle with two reheat stages and seven stages of feed-water heating. The superheater and the reheaters are arranged in series. The total thermal power in this cycle is 2170 MWt, and the gross thermal efficiency of this cycle is 46.5%.

The main results and parameters of the first-wall and divertor cycle and the IBC and shield cycle are given in Table 9.7-I. The overall gross thermal efficiency for the TITAN-I design, by combining the efficiencies of the two cycles, is 44%.

9.8. DIVERTOR ENGINEERING

The design of the impurity-control system poses some of the most severe problems of any component of a DT fusion reactor and for a compact or high-power-density device these problems can be particularly challenging. The final TITAN-I divertor design represents the result of extensive iterations between edge-plasma analysis, magnetic design, thermal-hydraulic and structural analysis, and neutronics.

A summary of the results of the edge-plasma modeling is given in Table 9.8-I and is described in detail in Section 5.4. The plasma power flow is controlled by the injection of a trace amount of a high- Z material (xenon) into the plasma which causes strong radiation from the core, scrape-off layer, and divertor plasmas. About 95% of the steady-state heating power (alpha particle and ohmic heating by the current-drive system) is thereby radiated to the first wall and divertor plate, although only about 70% is radiated from the core plasma (*i.e.*, inside the separatrix). This intense radiation reduces the power deposited on the divertor target by the plasma to an acceptably low level. Preliminary experimental results [12,13] suggest that beta-limited RFP plasmas can withstand a high fraction of power radiated without seriously affecting the global confinement (Section 5.3). The radiative cooling also reduces the electron temperature at the first wall and divertor target (also assisted by recycling) which, in turn, reduces the sputtering and erosion problems.

To satisfy the requirement for a high- Z material for the plasma-facing surface of the divertor target, a tungsten-rhenium alloy (W-26Re) is used. The high rhenium content provides the high ductility and high strength necessary for the severe loading conditions. A bank of lithium-cooled vanadium-alloy coolant tubes removes the heat deposited on the target. These tubes are separated from the tungsten-alloy armor by a thin, electrically insulating layer of spinel, to avoid an excessive MHD pressure drop. Fabrication of the divertor target is based on brazing the tungsten-alloy plate (produced by powder-metallurgy techniques) to the bank of coolant tubes, with the spinel layer deposited by the chemical-vapor-deposition (CVD) process. As a second technique, a unique manufacturing process using CVD (instead of brazing) is proposed to enhance bond strength of the tungsten-spinel-vanadium interfaces.

Table 9.7-I.

PARAMETERS OF THE TITAN-I POWER CYCLE

First-Wall and Divertor Power Cycle:		
Total thermal power in the primary coolant	765	MWt
Primary-coolant inlet temperatures	320	°C
Primary-coolant exit temperatures	442	°C
Secondary-coolant inlet temperatures	300	°C
Secondary-coolant exit temperatures	422	°C
Throttle steam temperature	396	°C
Throttle steam pressure	10.7	MPa
Steam flow rate	326	kg/s
Condenser back pressure	6.76×10^3	Pa
Stages of feed-water heating	4	
Feed-water inlet temperature	169	°C
Gross thermal efficiency	37.0%	
IBC and Shield Power Cycle:		
Total thermal power in the primary coolant	2170	MWt
Primary-coolant inlet temperatures	320	°C
Primary-coolant exit temperatures	700	°C
Secondary-coolant inlet temperatures	300	°C
Secondary-coolant exit temperatures	680	°C
Steam temperature after 1st reheat	565.6	°C
Steam temperature after 2nd reheat	550.0	°C
Throttle steam pressure	21.4	MPa
Steam flow rate	703	kg/s
Condenser back pressure	6.76×10^3	Pa
Stages of feed-water heating	7	
Feed-water inlet temperature	258	°C
Gross thermal efficiency	46.5%	
Overall gross thermal efficiency	44.0%	

Table 9.8-I.
SUMMARY OF TITAN-I EDGE-PLASMA CONDITIONS

Number of divertors	3	
Scrape-off layer thickness	6	cm
Peak edge density	1.7×10^{20}	m^{-3}
Peak edge ion temperature	380	eV
Peak edge electron temperature	220	eV
Plasma temperature at first wall	1.7	eV
Peak divertor density	6×10^{21}	m^{-3}
Peak divertor plasma temperature	4.5	eV
Divertor recycling coefficient	0.995	
Throughput of DT	6.7×10^{21}	s^{-1}
Throughput of He	8.2×10^{20}	s^{-1}
Vacuum tank pressure	20	mtorr

The TITAN-I impurity-control system is based on the use of toroidal-field divertors to minimize the perturbation to the global magnetic configuration (toroidal-field is the minority field in RFPs) and to minimize the coil currents and stresses. The TITAN divertor uses an “open” configuration, in which the divertor target is located close to the null point and faces the plasma, rather than in a separate chamber. This positioning takes advantage of the increased separation between the magnetic field lines (flux expansion) in this region, which tends to reduce the heat loading on the divertor plate because the plasma flowing to the target is “tied” to the field lines. The high plasma density in front of the divertor target ensures that the neutral particles emitted from the surface have a short mean free path; a negligible fraction of these neutral particles enter the core plasma (Section 5.5).

The final magnetic design includes three divertor modules, located 120° apart in toroidal direction (Figure 9.8-1). The magnetic field lines are diverted onto the divertor

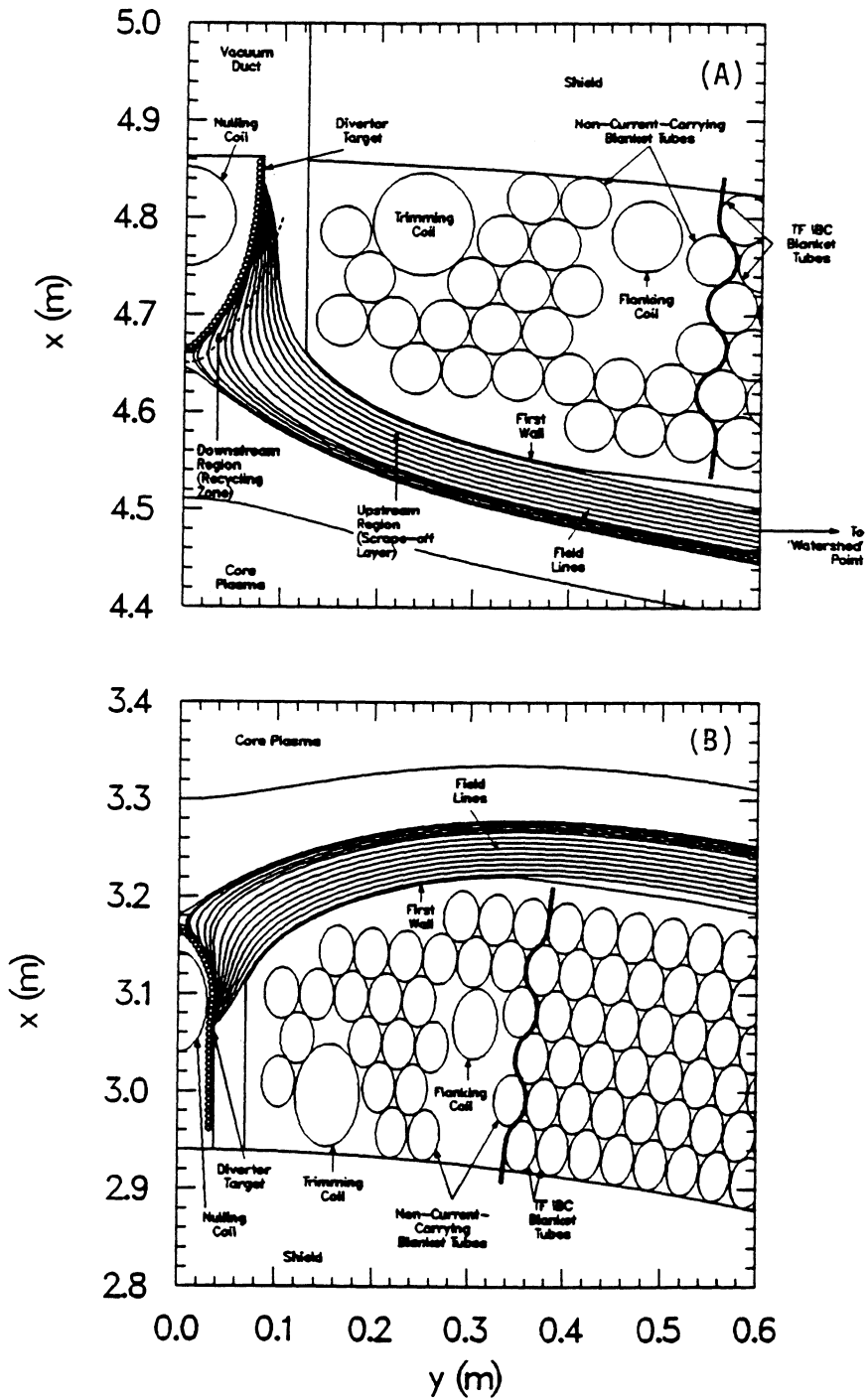


Figure 9.8-1. Outboard (A) and inboard (B) equatorial-plane views of the divertor region for TITAN-I.

plate using a nulling coil and two flanking coils which localize the nulling effect. For the TITAN-I design, the divertor IBC assembly displaces a part of the TF IBC tube bank. Therefore, a pair of trim coils is also required to control the toroidal-field ripple. Also shown on the outboard view of Figure 9.8-1 is the pumping aperture which leads to the vacuum tank surrounding the torus. This aperture is present for only the outboard 90° in the poloidal angle; elsewhere there is shielding material to protect the OH coils.

The low value of the toroidal field in the RFP allows high coolant velocities to be achieved without prohibitive MHD pressure drops, thus permitting operation in the turbulent flow regime with the associated high heat-transfer coefficients. Despite the intense radiation arising from the impurities injected into the plasma, careful shaping of the divertor target, as shown in Figure 9.8-1, is also required to maintain the heat flux at acceptable levels at all points on the plate. Figure 9.8-2 shows the distribution of the various components of the surface heat flux along the divertor target for the inboard and outboard locations. The heat flux on the inboard target ($\sim 9.5 \text{ MW/m}^2$) is significantly higher than that on the outboard ($\sim 6 \text{ MW/m}^2$), because of the toroidal effects.

The temperature distribution of the target plate coolant and structure is shown in Figure 9.8-3. The same coolant inlet temperature of 320°C as for the first wall is used, allowing both coolant loops to be fed from the same circuit. The maximum temperature of the vanadium-alloy tubes does not exceed 750°C . The maximum temperature of the tungsten-rhenium armor is about 930°C , at which level the alloy retains high strength and the thermal stresses are within allowable levels.

A total pressure drop of 12 MPa was used for the divertor-coolant circuit. The maximum allowable coolant velocity was set at 25 m/s for this analysis, based on considerations of physical erosion. Figure 9.8-3 also shows the components of the pressure drop in the divertor-coolant tubes. Flow orificing is used extensively to tailor the coolant velocity distribution. In low-field regions, the large pressure head of 12 MPa would otherwise cause the velocity to exceed the 25 m/s limit. Near the outside of the plate, orificing allows the coolant outlet temperature to be adjusted so as to maintain an approximately constant level across the plate.

A detailed finite-element analysis of the steady-state temperatures and stresses in the divertor was made using the finite-element code, ANSYS [26], which has verified the design of the target plates (Section 11.5). A 2-D finite-element structural analysis also indicated that stress concentrations will occur at the edge of the interface between the different materials of the target. This aspect requires further analysis and experimental investigation to assure the viability of the design.

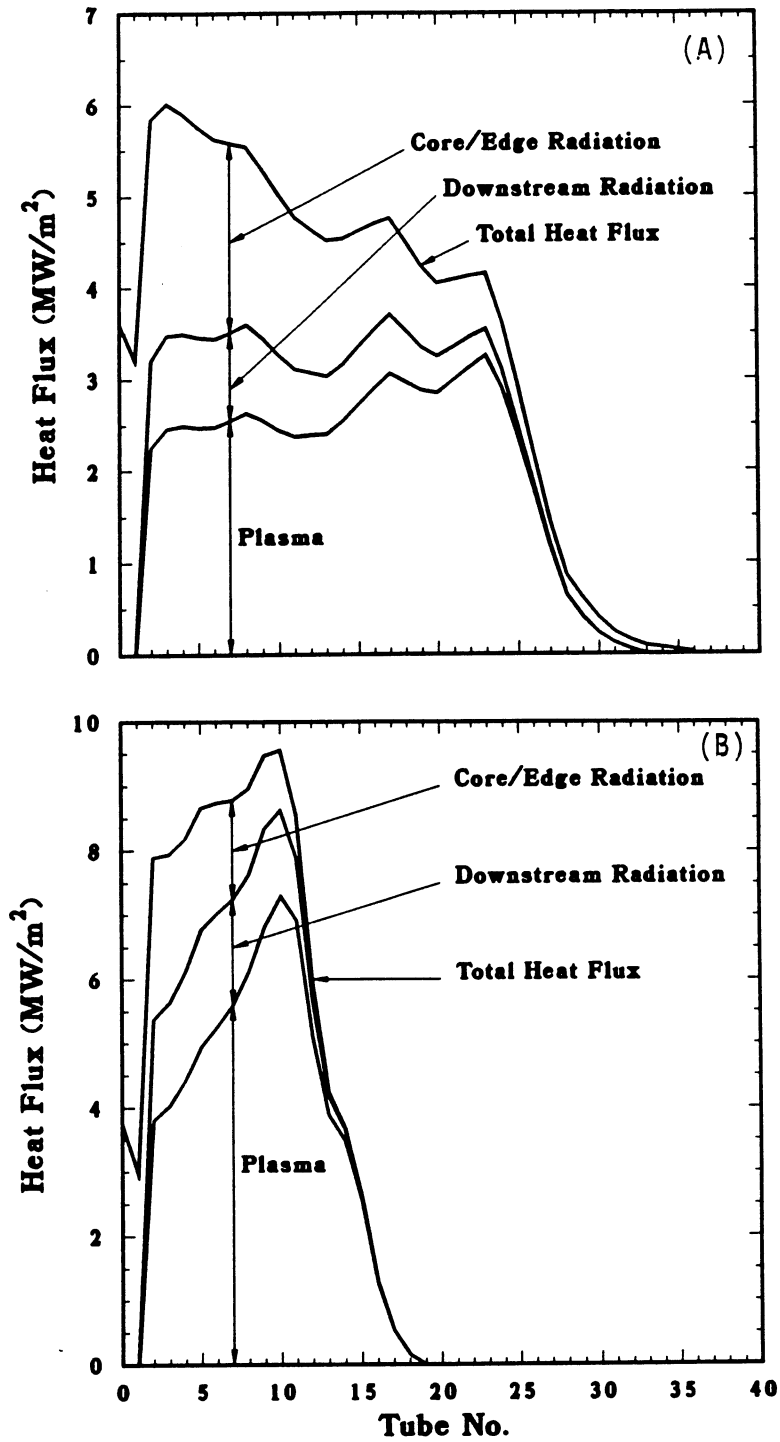


Figure 9.8-2. Heat flux distribution on outboard (A) and inboard (B) sections of divertor target. Coolant tubes are numbered from the apex or symmetry point of the target between the nulling coil and the core plasma.

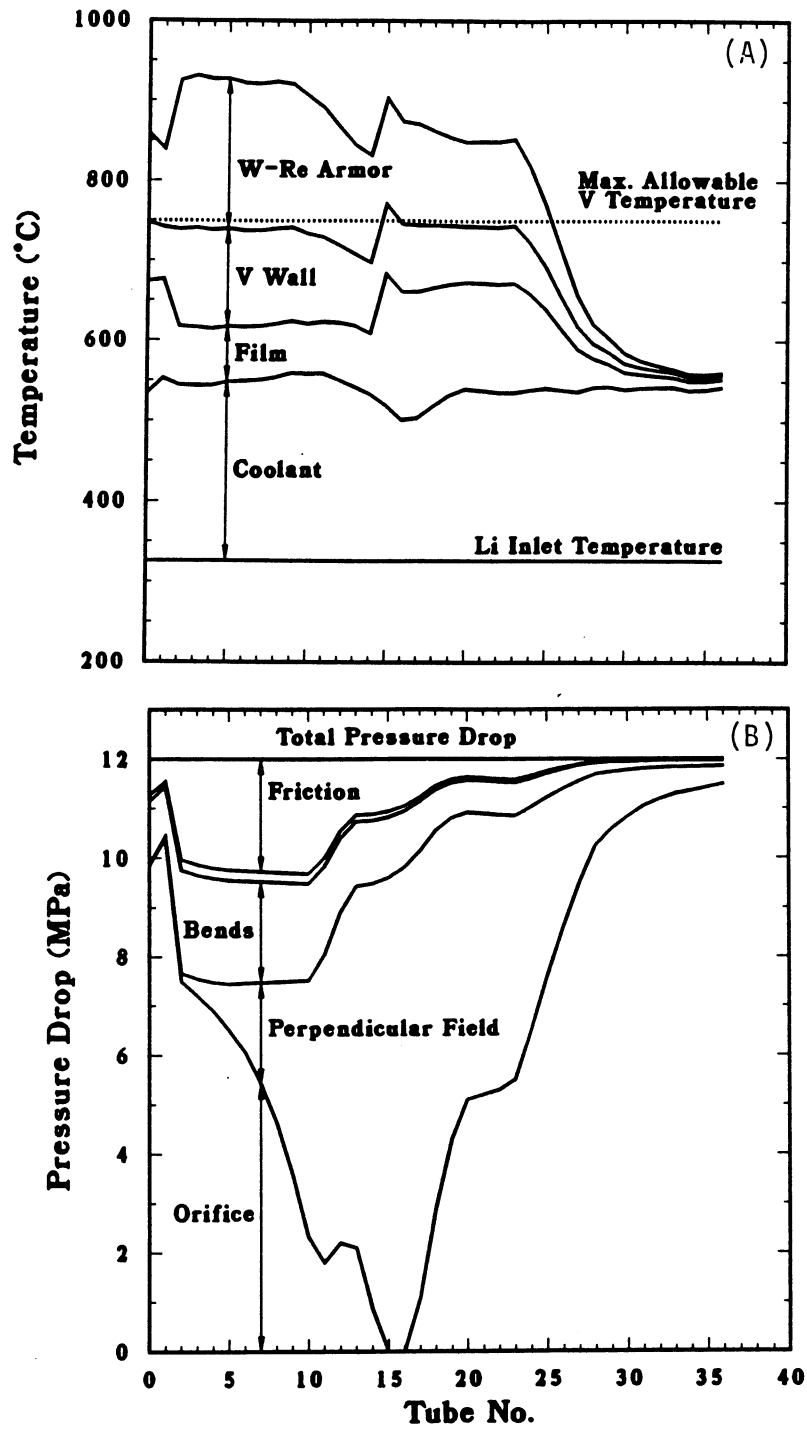


Figure 9.8-3. Coolant and structural temperatures at the coolant outlet (A) and components of the coolant pressure drop (B) for coolant tubes in the divertor target. Coolant tubes are numbered from the apex or symmetry point of the target between the nulling coil and the core plasma.

The vacuum system is based on the use of a large vacuum tank encompassing the entire torus, and connected to the divertor region by a duct located at each of the three divertor locations. It is proposed to employ lubricant-free magnetic-suspension-bearing turbo-molecular pumps for the high-vacuum pumps to avoid the possibility of tritium contamination of oil lubricants.

9.9. TRITIUM SYSTEMS

The major units in the tritium system of a fusion reactor are: (1) the plasma-processing system, (2) the breeder tritium-recovery system, (3) the atmospheric-tritium system, and (4) the secondary containment systems. The complete tritium system has to be designed under the constraints of tritium inventory, system cost, and tritium leakage rate. Significant relaxation of any one of the constraints will have a major impact on the overall design of the complete system.

In the TITAN design, the separation of the D and T of the plasma exhaust is not required. Therefore, only about 1% of the plasma exhaust will be required to pass through the cryogenic distillation system to separate protium generated by the DD reaction. The capacity and cost of the plasma-exhaust processing is thus much reduced. Since the cost of the plasma-exhaust-processing system is so low, a redundant unit is affordable. A double plasma-exhaust-processing system can significantly improve the reliability of the system and the reactor tritium storage can be reduced.

A molten-salt recovery process [28] is selected for tritium recovery from the lithium blanket, in which the liquid lithium and a molten salt are in contact, and LiH is preferentially distributed to the salt phase. The salt is then electrolyzed to yield hydrogen which is removed by sweeping the porous stainless-steel hydrogen electrode with a circulating stream of inert gas. The tritium is subsequently recovered from the inert gas with a getter. The molten-salt recovery process has been demonstrated on a laboratory scale to recover tritium from lithium down to 1 wppm. Therefore, the tritium inventory in the blanket would be moderate. The parameters of TITAN-I blanket tritium-recovery system is shown in Table 9.9-I.

Most reactor designs selected sodium as the intermediate coolant [16]. For the TITAN-I design, lithium is also used as the intermediate coolant to avoid using two separate technologies (sodium and lithium). Since, tritium solubility is much higher in lithium than in sodium, the TITAN-I design has a moderate amount of tritium inventory in the secondary loop. A unique advantage of using lithium as the primary coolant and

Table 9.9-I.
ANALYSIS OF MOLTEN-SALT EXTRACTION SCHEME FOR
A LIQUID-LITHIUM BLANKET SYSTEM

	Breeding rate	420 g/d ^(a)															
	Recovery rate	520 g/d ^(a)															
	Lithium exit temperature	556 °C ^(b)															
	Extraction system temperature	556 °C ^(b)															
Estimated blanket inventories																	
	Lithium	2.12 × 10 ⁸ g															
	Tritium	212 g (1 wppm)															
	Tritium recovery efficiency, ϵ	90%															
	Capacity per extractor unit	23 m ³ /h															
	Electrical power per unit	3.7 kW															
<table style="width: 100%; border-collapse: collapse;"> <thead> <tr> <th style="width: 20%; text-align: center;">Tritium Concentration (wppm)</th> <th style="width: 20%; text-align: center;">Effective Distribution Coefficient ($D_v\eta$)</th> <th style="width: 20%; text-align: center;">Lithium Processed per Hour (kg/h)</th> <th style="width: 20%; text-align: center;">Number of Units</th> <th style="width: 20%; text-align: center;">Required Electrical Power (kW)</th> </tr> </thead> <tbody> <tr> <td style="text-align: center;">1</td> <td style="text-align: center;">4</td> <td style="text-align: center;">22,000</td> <td style="text-align: center;">7</td> <td style="text-align: center;">26</td> </tr> <tr> <td style="text-align: center;">1</td> <td style="text-align: center;">1</td> <td style="text-align: center;">88,000</td> <td style="text-align: center;">28</td> <td style="text-align: center;">104^(c)</td> </tr> </tbody> </table>			Tritium Concentration (wppm)	Effective Distribution Coefficient ($D_v\eta$)	Lithium Processed per Hour (kg/h)	Number of Units	Required Electrical Power (kW)	1	4	22,000	7	26	1	1	88,000	28	104 ^(c)
Tritium Concentration (wppm)	Effective Distribution Coefficient ($D_v\eta$)	Lithium Processed per Hour (kg/h)	Number of Units	Required Electrical Power (kW)													
1	4	22,000	7	26													
1	1	88,000	28	104 ^(c)													

(a) Based on a tritium-breeding ratio of 1.2 and 100 g/d of PDP.

(b) Parameters of the Scoping Phase design,
the blanket and first-wall coolant were mixed in the outlet.

(c) Reference case.

Table 9.9-II.
TRITIUM INVENTORIES IN TITAN-I REACTOR

Unit	Tritium Inventory (g)
Storage	1,100
Primary-coolant loop	212
Secondary-coolant loop	300
Molten-salt extraction	10
Fuel processing	20
First wall:	
typical case	0.72
excessive PDP	4.53
Integrated blanket coil	2.20
Hot shield, zone 1	0.14
Hot shield, zone 2	0.25
Divertor shield	0.08
Divertor	< 0.01
Out-of-blanket piping	≪ 0.01
 Total TITAN-I inventory	 1,650

as the breeder is associated with the high tritium solubility in the lithium. The tritium partial pressure is very low. For a tritium concentration of 1 wppm, the tritium partial pressure is only 10^{-7} Pa. With such low tritium partial pressure, tritium containment is usually not a severe problem. This reduces the required capacity of the room-air-detritiation system and the secondary containment systems. The tritium inventories in TITAN-I components are shown in Table 9.9-II. The TITAN-I tritium inventory (1650 g) and leakage rate (7 Ci/d) are very reasonable.

A potential problem facing TITAN-I is the plasma-driven permeation (PDP) of low-energy tritons through the permeable vanadium-alloy first wall. The extent of PDP depends on the ability of the small fraction of high-energy plasma ions to adequately clean the first-wall surface, which is uncertain. The problem of PDP is not unique to

compact RFP designs. Any fusion reactor design with a combination of a low edge temperature and a vanadium-alloy first wall must consider this problem. Experiments are needed to determine the extent of PDP and the sputtering rate of the first-wall structure at low edge-plasma temperatures. In the TITAN-I design, a tungsten-rhenium alloy (W-26Re) is chosen for the divertor plates. Because tungsten is very resistant to permeation, PDP through the divertor plate is not a concern.

9.10. SAFETY DESIGN

Strong emphasis has been given to safety engineering in the TITAN study. Instead of an add-on safety design and analysis task, the safety activity was incorporated into the process of design selection and integration from the beginning of the study. The safety-design objectives of the TITAN-I design are: (1) to satisfy all safety-design criteria as specified by the U. S. Nuclear Regulatory Commission on accidental releases, occupational doses, and routine effluents; and (2) to aim for the best possible level of passive safety assurance.

The elevation view of the TITAN-I reactor is shown in Figure 9.2-1. The key safety features of the lithium self-cooled TITAN-I design are:

- The selection of a low-afterheat structural material, V-3Ti-1Si;
- The selection of a relatively high ${}^6\text{Li}$ enrichment (30%) to aid in further reducing afterheat and radioactive wastes;
- The use of three enclosures separating the lithium and air: the blanket tubes, vacuum vessel, and the containment building which is filled with argon cover gas;
- Locating all coolant piping connections at the top of the torus to prevent a complete loss of coolant in the FPC in case of a pipe break;
- The use of lithium-drain tanks to reduce the vulnerable lithium inventory should a pipe break occur;
- The use of steel liner to cover the containment-building floor to minimize the probability of lithium-concrete reaction;
- Excluding water from the containment building and vacuum vessel to prevent the possibility of lithium-water reaction.

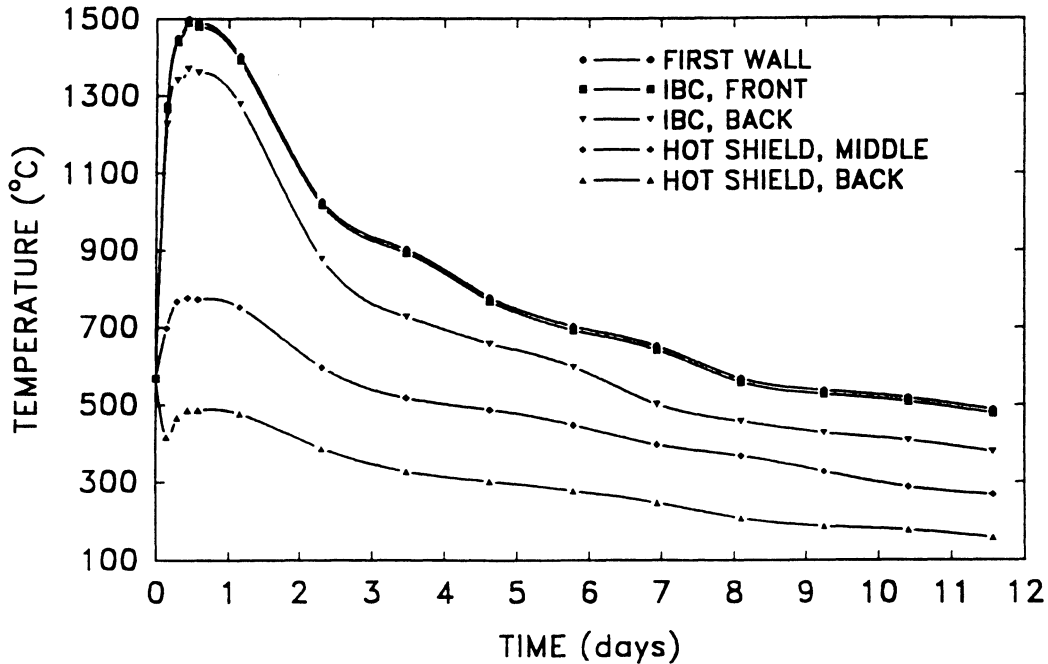


Figure 9.10-1. The thermal response of the TITAN-I FPC to a complete LOFA as a function of time after the initiation of the accident.

Two of the major accidents postulated for the fusion power core are the loss-of-flow accident (LOFA) and the loss-of-coolant accident (LOCA). Thermal responses of the TITAN-I FPC to these accidents are modeled using a finite-element heat-conduction code, TACO2D [29]. Figure 9.10-1 shows the resulting temperatures during a LOFA. At 12.8 hours after the initiation of the accident, the first wall reaches its peak temperature of 990°C which is well below the recrystallization temperature of the V-3Ti-1Si alloy. The first-wall peak temperature is also well below $\sim 1300^\circ\text{C}$, the on-set of volatilization of radioactive products (CaO, SrO) in the vanadium alloy (more experimental data is needed to clarify the on-set temperature and the extent of the release of these radioisotopes). The heat capacity of the static lithium accounts for the moderate temperature excursion. No natural convection of the coolant is assumed even though the emergency plasma shutdown procedure is accompanied by the discharge of all magnets and no MHD retarding force is expected on the coolant. If natural convection develops, the temperature excursions would be considerably smaller than those predicted by Figure 9.10-1.

Thermal creep-rupture behavior of the TITAN-I first wall during accidents is estimated using the modified-minimum-commitment method (MMCM) [18]. For the materials and loadings expected in the TITAN-I first wall during a LOFA, the thermal stresses

have a negligible influence on the rupture time relative to the pressure stresses. The predicted rupture times for several primary stresses at 1000°C are given in Table 9.10-I. Since the coolant pressure is lost during off-normal conditions, the expected primary stress in the TITAN-I design during a LOFA is below 2 MPa and is caused by the hydrostatic pressure load inside the coolant piping. Table 9.10-I shows that creep-rupture would not occur even if the structure is kept at elevated temperatures (1000°C) for a prolonged period of time – a LOFA would not lead to a LOCA. High-temperature creep-rupture data above 850°C are necessary to gain more confidence in the creep-rupture behavior at these higher temperatures.

Higher afterheat is expected in the tungsten plate of the divertor. During a LOFA, the peak temperature in the divertor vanadium cooling tube is 1117°C, close to recrystallization temperature of the V-3Ti-1Si. This may result in shortening the lifetime of the divertor modules, but failure that would lead to a LOCA is unlikely.

In the event of major primary-pipe breaks and failure of the containment building and vacuum vessel, air could enter the vacuum chamber and start a lithium fire. The TITAN-I reactor is configured so as (1) to ensure that a lithium fire would be a low probability event, and (2) to minimize the consequences of lithium fire if it occurs. In order to reduce the probability of lithium fires, three barriers (primary-coolant pipes, the vacuum tank, and the containment building) exist between the primary-coolant lithium and air. The containment building is also filled with argon cover gas. In order to reduce

Table 9.10-I.

CREEP-RUPTURE TIME FOR TITAN-I FIRST WALL

Primary Stress, σ_p (MPa)	Rupture Time, t_r (h)
10	3200
20	360
30	101
40	41
50	20

the consequences of a lithium spill, two sets of lithium-drain tanks are provided to drain the maximum amount of lithium in less than 30 seconds.

For the perceived worst-accident condition of a lithium fire with breach of all barriers and no argon cover gas, the maximum combustion-zone temperature is found to be less than 1000 °C. The tritium release in this case would be about 60 Ci which is quite acceptable under this worst-accident scenario. Of critical concern in the lithium-fire scenario is the formation and release of vanadium oxide V_2O_5 . Further measurement of vanadium-oxide formation and its vapor pressure with temperature, and the calculation of potential releases to the public based on the TITAN-I configuration and accident scenarios should be performed.

The total tritium inventories in the lithium primary and secondary loops are 344 and 300 g, respectively. These are acceptable inventories when passive drain tanks are used to control the amount of possible tritium releases. The tritium inventory in the blanket structure is less than 10 g, which is also acceptable. The tritium-leakage rate from the primary loop was estimated to be 7 Ci/d which is within the 10 Ci/d design goal.

Plasma-accident scenarios need to be further evaluated as the physics behavior of RFPs becomes better understood. Preliminary results indicate that passive safety features can be incorporated into the design, such that the accidental release of plasma and magnetic energies can be distributed without leading to major releases of radioactivity. Research activities in this area need to be continued, especially for high-power-density devices.

Based on the analyses summarized above, TITAN-I does not need to rely on any active safety systems to protect the public. A LOFA will result in no radioactive release and will not lead to a more serious LOCA. A complete LOCA from credible events is not possible. Only the assurance of coolant-piping and vacuum-vessel integrity is necessary to protect the public. The TITAN-I design, therefore, meets the definition of level 3 of safety assurance, "small-scale passive safety assurance" [30,31]. Pending information on the vanadium-oxide formation and release from the TITAN-I vacuum chamber under the lithium-fire accident scenario, the qualification of TITAN-I as a level-2 of safety assurance design, "large-scale passive safety assurance," may also be possible.

9.11. WASTE DISPOSAL

The neutron fluxes calculated for the reference TITAN-I reactor were used as input to the activation calculation code, REAC [32]. These results were analyzed to obtain the

allowable concentrations of alloying and impurity elements in TITAN-I FPC components. Waste-disposal analysis has shown that the compact, high-power density TITAN-I reactor can be designed to meet the criteria for Class-C waste disposal [33]. The key features in achieving Class-C waste in the TITAN-I reactor are attributed to: (1) materials selection and (2) control of impurity elements.

The materials selected for the TITAN-I FPC are the vanadium alloy, V-3Ti-1Si, and lithium. The main alloying elements of V-3Ti-1Si do not produce long-lived radionuclides with activity levels exceeding the limits for Class-C disposal (no limit on the concentration of vanadium and titanium and 23% allowable concentration of silicon which is much larger

Table 9.11-I.

**MAXIMUM CONCENTRATION LEVELS OF IMPURITIES IN TITAN-I
REACTOR COMPONENTS TO QUALIFY AS CLASS-C WASTE**

Element	Major Nuclide (Activity Limit) ^(a)	Components			Nominal Level
		FW & Blanket (1 FPY) ^(b)	Hot Shield (5 FPY) ^(b)	OH Magnets (30 FPY) ^(b)	
Nb (appm)	⁹⁴ Nb (0.2 Ci/m ³)	5.	1.4	0.5	0.1
Mo (appm)	⁹⁹ Tc (0.2 Ci/m ³) ⁹⁴ Nb (0.2 Ci/m ³)	65.	100.	90.	1.0
Ag (appm)	^{108m} Ag (3 Ci/m ³)	1.3	1.5	0.7	1.0
Tb (appm)	¹⁵⁸ Tb (4 Ci/m ³)	0.4	0.6	7.0	5.0
Ir (appm)	^{192m} Ir (2 Ci/m ³)	0.1	0.1	0.02	5.0
W	^{186m} Re (9 Ci/m ³)	5%	9%	100%	0.89%

(a) From Reference [32].

(b) Based on operation at 18 MW/m² of neutron wall loading.

than 1% content of Si in V-3Ti-1Si). The allowable concentrations of various impurities in the vanadium structural material of the TITAN-I reactor are listed in Table 9.11-I. Some of these impurity elements, mainly niobium and possibly silver, terbium, and iridium, need to be controlled in the vanadium alloy below appm levels.

Table 9.11-II summarizes the TITAN materials and related quantities for Class-C disposal. The total weight in the FPC of the TITAN-I reactor is about 1363 tonnes, of which about 73% is from the magnet systems (OH and EF coils, and EF shield) that last the plant lifetime. The reactor torus (first wall, blanket, and the divertor module) is replaced annually and constitutes only 4% of the total weight of the FPC. The balance of the weight is from the shield which has a five-year lifetime. The average annual-replacement mass of the FPC is about 150 tonnes.

The TITAN-I divertor plates are fabricated with a tungsten armor because of its low sputtering properties. The waste-disposal rating of the divertor plates is estimated to be a factor of 10 higher than for Class-C disposal after one year of operation. The annual disposal mass of this non-Class-C waste is 0.35 tonnes, about 0.23% of the average annual discharge mass.

The conclusions derived from the TITAN-I reactor study are general, and provide strong indications that Class-C waste disposal can be achieved for other high-power-density approaches to fusion. These conclusions also depend on the acceptance of recent evaluations of specific activity limits carried out under 10CFR61 methodologies [34].

9.12. MAINTENANCE

The TITAN reactors are compact, high-power-density designs. The small physical size of these reactors permits each design to be made of only a few pieces, allowing a single-piece maintenance approach [7,8]. Single-piece maintenance refers to a procedure in which all of components that must be changed during the scheduled maintenance are replaced as a single unit, although the actual maintenance procedure may involve the movement, storage, and reinstallation of some other reactor components. In TITAN designs, the entire reactor torus is replaced as a single unit during scheduled maintenance. Furthermore, because of the small physical size and mass of the TITAN-I FPC, the maintenance procedures can be carried out through vertical lifts, allowing a much smaller reactor vault.

Table 9.11-II.

**SUMMARY OF TITAN-I REACTOR MATERIALS AND RELATED
WASTE QUANTITIES FOR CLASS-C WASTE DISPOSAL^(a)**

Component	Material	Lifetime (FPY)	Volume (m ³)	Weight (tonnes)	Annual Replacement Mass (tonnes/FPY)
First wall	V-3Ti-1Si	1	0.4	2.5	2.5
Blanket (IBC)	V-3Ti-1Si	1	6.4	39.2	39.2
Shield (zone 1)	V-3Ti-1Si	5	15.5	95.6	19.1
Shield (zone 2)	V-3Ti-1Si	5	28.0	172.0	34.4
OH coils	Modified steel	30	3.8	34.0	1.1
	Copper		26.6	239.0	8.0
	Spinel		3.8	15.2	0.5
	TOTAL		34.2	289.2	9.6
EF coils	Modified steel	30	43.0	315.0	10.5
EF shield	Modified steel	30	43.9	347.0	11.6
	B ₄ C		18.8	47.0	1.6
	TOTAL		62.7	394.0	13.2
Divertor shield					
zone 1	V-3Ti-1Si	1	2.3	14.2	14.2
zone 2	V-3Ti-1Si	5	6.7	41.2	8.2
TOTAL CLASS-C WASTE			199.	1363.	151.

(a) Based on operation at 18 MW/m² of neutron wall loading.

Potential advantages of single-piece maintenance procedures are identified:

1. Shortest period of downtime resulting from scheduled and unscheduled FPC repairs;
2. Improved reliability resulting from integrated FPC pretesting in an on-site, non-nuclear test facility where coolant leaks, coil alignment, thermal-expansion effects, *etc.*, would be corrected by using rapid and inexpensive hands-on repair procedures prior to committing the FPC to nuclear service;
3. No adverse effects resulting from the interaction of new materials operating in parallel with radiation-exposed materials;
4. Ability to modify continually the FPC as may be indicated or desired by reactor performance and technological developments; and
5. Recovery from unscheduled events would be more standard and rapid. The entire reactor torus is replaced and the reactor is brought back on line with the repair work being performed, afterwards, outside the reactor vault.

The lifetime of the TITAN-I reactor torus (first wall, blanket, and divertor modules) is estimated to be in the range of 15 to 18 MWy/m², and the more conservative value of 15 MWy/m² will require the change-out of the reactor torus on a yearly basis for operation at 18 MW/m² of neutron wall loading at 76% availability. The lifetime of the hot shield is estimated to be 5 years and, therefore, to reduce the rad-waste, the TITAN-I hot shield is made of two pieces with the upper hot shield removed during the maintenance procedures and reused in the next replacement of the reactor torus.

Seventeen principal tasks must be accomplished for the annual, scheduled maintenance of the TITAN-I FPC. These steps are listed in Table 9.12-I. The tasks which would require a longer time to complete in a modular design are also identified in Table 9.12-I (assuming the same configuration for the modular design as that of TITAN-I). Vertical lifts have been chosen for the component movements during maintenance. Lift limits for conventional bridge cranes is around 500 tonnes, with special-order crane capacities in excess of 1000 tonnes. The most massive components lifted during TITAN-I maintenance are the upper OH-coil set (OH coils 2 through 5) and the upper hot shield each weighing about 150 tonnes, which are easily manageable by the conventional cranes. The four major component lifts are illustrated in Figure 9.12-1.

An important feature of the TITAN design is the pretest facility. This facility allows the plant personnel to test fully the new torus assemblies in a non-nuclear environment

Table 9.12-I.
PRINCIPAL TASKS
DURING THE TITAN-I MAINTENANCE PROCEDURE

1. Orderly shutdown of the plasma and discharge of the magnets;
2. Continue cooling the FPC at a reduced level until the decay heat is sufficiently low to allow cooling by natural convection in the argon atmosphere;
3. During the cool-down period:
 - a. Continue vacuum pumping until sufficient tritium is removed from the FPC,
 - b. Break vacuum (valve-off vacuum pumps and cut weld at vacuum tank lid),^(a)
 - c. Remove vacuum-tank lid to the lay-down area,
 - d. Disconnect electrical and coolant supplies from the upper OH-coil set;
4. Drain lithium from the FPC;
5. Lift OH-coil set and store in the lay-down area;
6. Disconnect lithium-coolant supplies;^(a)
7. Lift upper shield and store in the lay-down area;
8. Lift the reactor torus and move to the hot cell;^(a)
9. Inspect FPC area;
10. Install the new, pretested torus assembly;^(a)
11. Connect lithium supplies;^(a)
12. Replace upper shield and connect shield-coolant supplies;
13. Replace the upper OH-coil set and connect electrical and coolant supplies;
14. Hot test the FPC;^(b)
15. Replace vacuum-tank lid and seal the vacuum tank;^(a)
16. Pump-down the system;^(c)
17. Initiate plasma operations.

(a) The time required to complete these tasks is likely to be longer for a modular system than for a single-piece system, assuming similar configuration.

(b) The new torus assembly is pretested and aligned before commitment to service. Only minimal hot testing would be required.

(c) The TITAN-I reactor building is filled with argon gas and the replacement torus is also stored in argon atmosphere. Therefore, the pump-down time would be short.

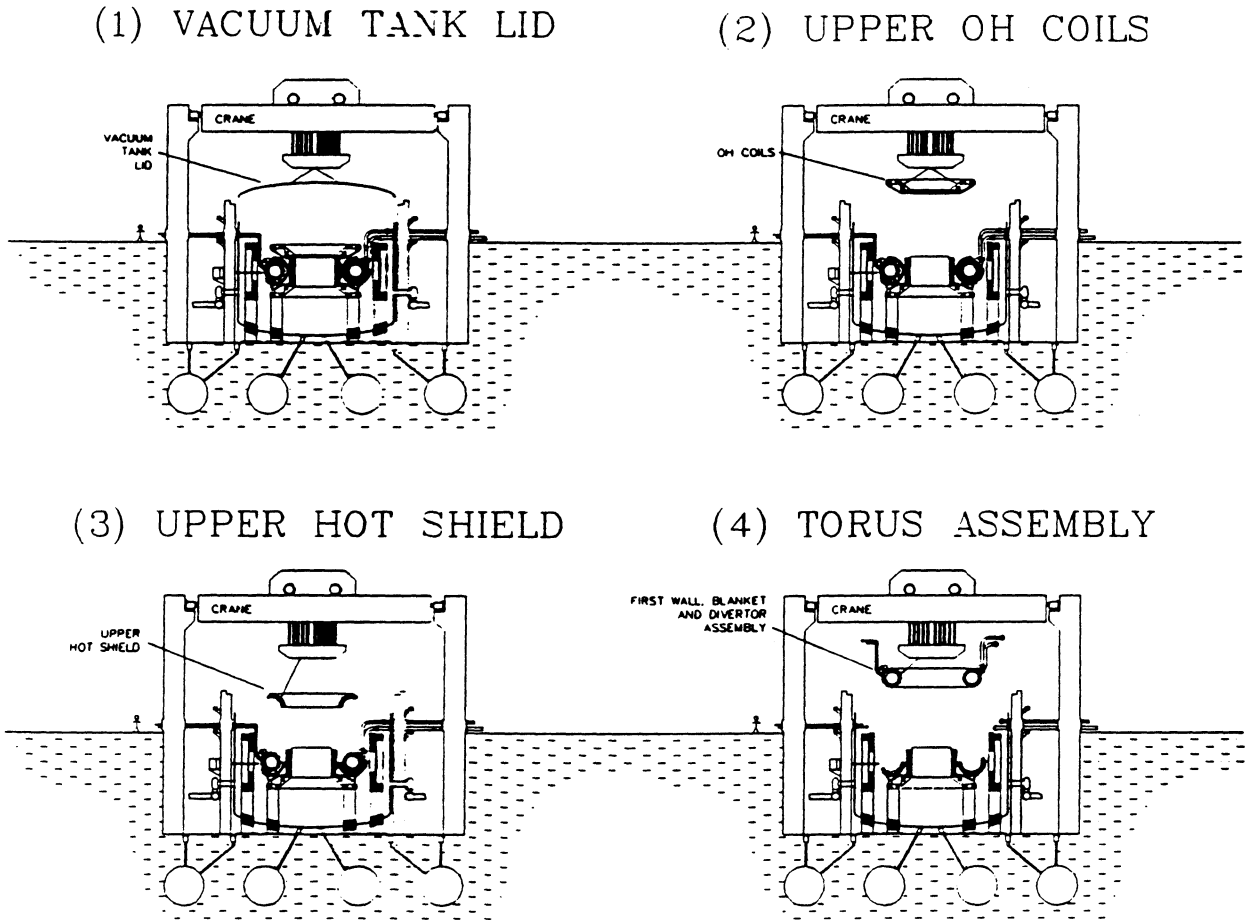


Figure 9.12-1. Four major crane lifts required for the TITAN-I maintenance.

prior to committing it to full-power operation in the reactor vault. Any faults discovered during pretesting can be quickly repaired using inexpensive hands-on maintenance. Furthermore, additional testing can be used as a shake-down period to reduce the infant mortality rate of the new assemblies. A comprehensive pretest program could greatly increase the reliability of the FPC, hence increasing the plant overall availability. The benefits of pretesting (higher reliability, higher availability) must be balanced with the additional cost associated with the pretest facility. The more representative the pretests are of the actual operation, the more duplication of the primary-loop components is required. A detailed list of pretests for the TITAN-I design is included in Table 9.12-II.

9.13. SUMMARY AND KEY TECHNICAL ISSUES

The TITAN reversed-field-pinch (RFP) fusion reactor study [1] is a multi-institutional research effort to determine the technical feasibility and key developmental issues for an RFP fusion reactor operating at high power density and to determine the potential economic (cost of electricity, COE), operational (maintenance and availability), safety, and environmental features of high mass-power-density (MPD) fusion systems.

Two different detailed designs, TITAN-I and TITAN-II, have been produced to demonstrate the possibility of multiple engineering design approaches to high-MPD reactors. Both designs would use RFP plasmas operating with essentially the same parameters. The major features of the designs are listed in Table 9.1-I. Both conceptual reactors are based on the DT fuel cycle, have a net electric output of about 1000 MWe, are compact and have a high MPD of about 800 kWe/tonne of FPC. The mass power density and the FPC power density of several fusion-reactor designs and a fission pressurized-water reactor (PWR) are shown in Figure 9.13-1 and compared with those of the TITAN reactors. The TITAN study further shows that with proper choice of materials and FPC configuration, compact reactors can be made passively safe and that the potential attractive safety and environmental features of fusion need not be sacrificed in compact reactors. The TITAN designs would meet the U. S. criteria for the near-surface disposal of radioactive waste (Class-C, 10CFR61) [33] and achieve a high level of safety assurance [30,31] with respect to FPC damage by decay afterheat and radioactivity release caused by accidents. Very importantly, a “single-piece” FPC maintenance procedure, unique to high MPD reactors, has been worked out and appears feasible for both designs.

Parametric system studies have been used to find cost-optimized designs, to determine the parametric design window associated with each approach, and to assess the sensitivity

Table 9.12-II.

MAIN PREOPERATIONAL TESTING OF THE TITAN-I FPC

Test	Sub-Module ^(a)	Module ^(a)	Full Torus ^(b)	
			No Plasma	Plasma ^(c)
Mechanical				
• Tube-bank vibration (first wall, blanket)	X	X	X	
• Tube-bank expansion (first wall, blanket)	X	X	X	
• Inter-module and full-torus deflection			X	
• Plasma chamber (shell)/coil displacement			X	
Thermal Hydraulic				
• Flow rates, pressure drops, leaks, ... :			X	
★ First wall, divertor, blanket, shield	X			
★ Coils			X	
★ Manifolds, headers			X	
• "Hot" FPC test, (pressure drops, vibrations, ...)			X	
★ Electrically heated coolant			X	
★ Plasma-driven heat fluxes				X
• Remote coupling, disconnects	X	X	X	
Electrical				
• Magnet test (forces, deflection, voltages, ...)			X	X
• Vacuum-field mapping (TF ripple, vertical field, ...)			X	
• Plasma transients				
★ RFP formation			X	X
★ Fast-ramp phase			X	X
★ Slow-ramp phase				X
• Current-drive (steady-state) phase				X
• Active feedback control			X	X
• Eddy currents (start-up, OFCD)				
★ First wall and shell			X	X
★ Blanket and shield			X	X
★ Coil casing, structure, pumps, ...			X	X
• Termination control/response				X
Vacuum, Fueling, and Impurity-Control Systems				
• Base vacuum			X	
• Full gas-load test			X	
• Pellet injection				X
Neutronics				
• Breeding efficiency				X
• Energy-recovery efficiency				X
• Shielding effectiveness, streaming				X

(a) Performed at factory site.

(b) Performed at plant site during operational year.

(c) Performed in the reactor vault during the scheduled maintenance.

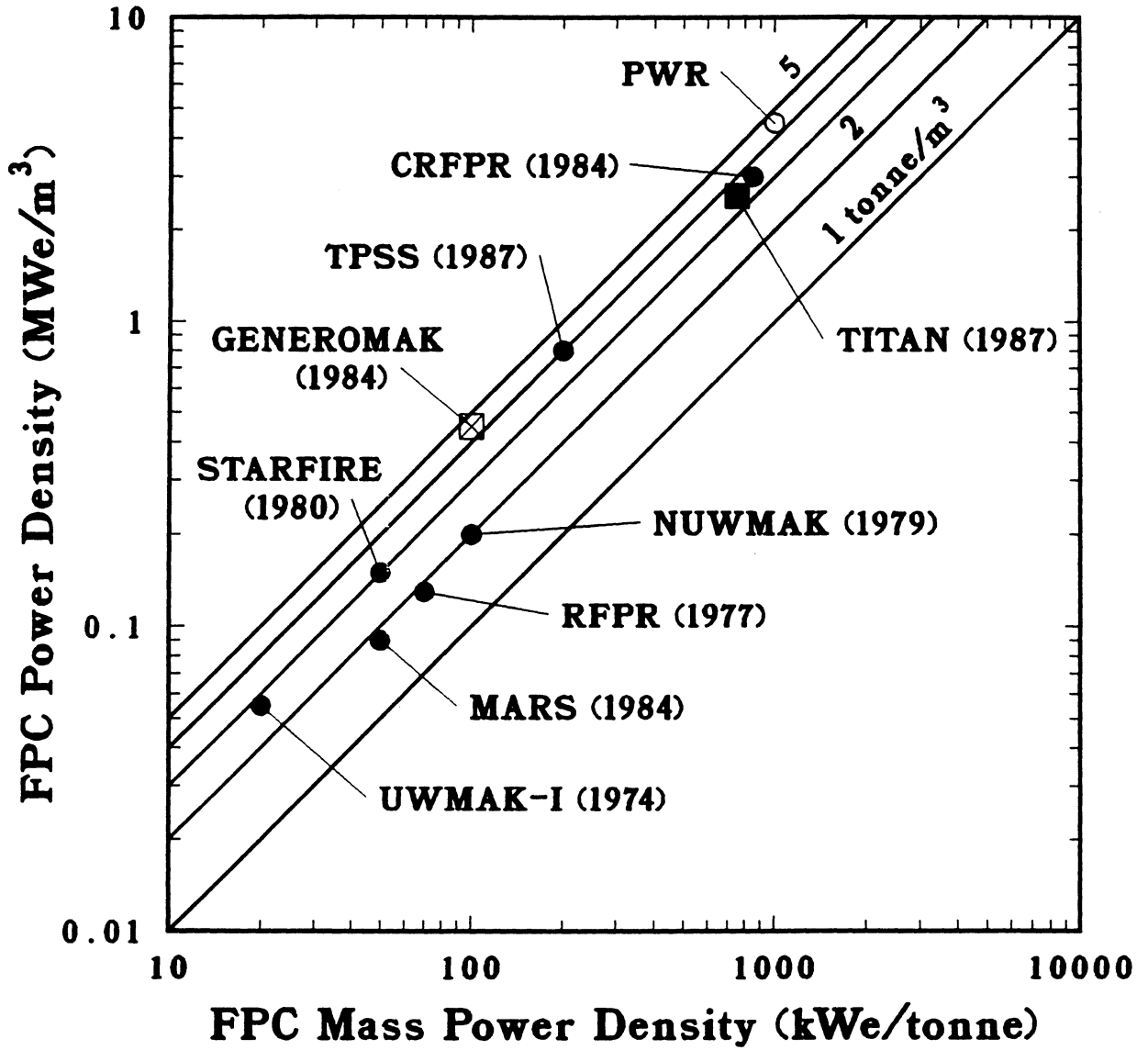


Figure 9.13-1. The MPD and the FPC power density of several fusion reactor designs, including TITAN, and a fission PWR.

of the designs to a wide range of physics and engineering requirements and assumptions. The design window for such compact RFP reactors would include machines with neutron wall loadings in the range of 10 to 20 MW/m² with a shallow minimum for COE at about 19 MW/m². The high MPD values possible for the RFP appear to be a unique attribute of this confinement concept [6]. Reactors in this “design window” are physically small and a potential benefit of this “compactness” is improved economics. Also, the cost of the FPC for TITAN reactors is a small fraction of the overall estimated plant cost (< 10%, similar to a fission PWR), making the economics of the reactor less sensitive to changes in the plasma performance or unit costs for FPC components. Moreover, since the FPC is smaller and cheaper, a development program should cost less. Even though operation at the lower end of the this design window of wall loading (10 to 12 MW/m²) is possible, and may be preferable, the TITAN study adopted the design point at the upper end (18 MW/m²) in order to quantify and assess the technical feasibility and physics limits for such high-MPD reactors.

The TITAN-I design is a lithium, self-cooled design with a vanadium alloy (V-3Ti-1Si) structural material. Magneto-hydrodynamics (MHD) effects had precluded the use of liquid-metal coolants for high-heat-flux components in previous designs (mainly of tokamaks), but the magnetic field topology of the RFP is favorable for liquid-metal cooling. In the TITAN-I design, the first wall and blanket consist of single pass, poloidal-flow loops aligned with the dominant poloidal magnetic field. Other major features are: separation of the first-wall and blanket coolant circuits to allow a lower coolant-exit temperature from the first wall; and use of MHD turbulent-flow heat transfer at the first wall, made possible by the low magnetic interaction parameter. The TITAN-I thermal-hydraulic design (Table 9.5-I) can accommodate up to 5 MW/m² of heat flux on the first wall with a reasonable MHD pressure drop, a high thermal-cycle efficiency, and a modest pumping power of about 45 MWe. A molten-salt tritium-extraction technique is used.

A unique feature of the TITAN-I design is the use of the integrated-blanket-coil (IBC) concept [14]. With the IBC concept, the lithium coolant in the blanket circuit flowing in the poloidal direction is also used as the electrical conductor of the toroidal-field and divertor coils. The IBC concept eliminates the need for shielding the coils and allows direct access to the blanket and shield assemblies, thereby easing the maintenance procedure.

The general arrangement of the TITAN-I reactor is illustrated in Figures 9.2-1 to 9.2-6. The operational (maintenance and availability), safety, and environmental issues have been taken into account throughout the design. For example, the entire FPC is contained in a vacuum tank to facilitate the remote making and breaking of vacuum

welds. All maintenance procedures would be performed by vertical lift of the components (heaviest component weighs about 250 tonnes), reducing the size of the expensive containment building. The compactness of the TITAN designs would reduce the FPC to a few small and relatively low-mass components, making toroidal segmentation unnecessary. A “single-piece” FPC maintenance procedure, in which the first wall and blanket are removed and replaced as a single unit is, therefore, possible. This unique approach permits the complete FPC to be made of a few factory-fabricated pieces, assembled on site into a single torus, and tested to full operational conditions before installation in the reactor vault. The low cost of the FPC means a complete, “ready-for-operation” unit can be kept on-site for replacement in case of unscheduled events. All of these features are expected to improve the plant availability.

All of the FPC primary-coolant ring-headers are located above the torus for ease of access during maintenance. This arrangement also ensures that the coolant will remain in the torus in the event of a break in the primary piping. The most severe safety event will be a loss-of-flow accident (LOFA). The FPC and the primary coolant loop are located in an inert-gas-filled (argon) confinement building which, together with the blanket containers and the vacuum vessel, form three barriers to prevent air influx, thereby reducing the hazards of lithium fires and providing protection for the public from radioactive materials. Lithium-drain tanks are provided for both the reactor vault and the vacuum tank to reduce passively the vulnerable blanket-lithium inventory.

A low-activation, low-after-heat vanadium alloy is used as the structural material throughout the FPC in order to minimize the peak temperature during a LOFA and to permit near-surface disposal of waste. The maximum temperature during a first-wall LOCA and system LOFA (the most severe accident postulated for TITAN-I) is 990 °C. Lithium-fire accident scenarios and site-boundary dose calculations were performed to understand the potential release of radioactivity under major accident and routine release conditions. The safety analysis indicates that the liquid-metal-cooled TITAN-I design can be classified as passively safe, without reliance on any active safety systems. A high level of safety assurance [30,31] for the compact TITAN-I design, therefore, is expected.

The results from the TITAN study support the technical feasibility, economic incentive, and operational attractiveness of compact, high mass-power-density RFP reactors. The road towards compact RFP reactors, however, contains major challenges and uncertainties, and many critical issues remain to be resolved. The TITAN study has identified the key physics and engineering issues which are central to achieving reactors with the features of TITAN-I and TITAN-II.

The experimental and theoretical bases for RFPs have grown rapidly during the last few years [6], but a large degree of extrapolation to TITAN-class reactors is still required. The degree of extrapolation is one to two orders of magnitude in plasma current and temperature and two to three orders of magnitude in energy confinement time. However, the TITAN plasma density, poloidal beta, and plasma current density all are close to present-day experimental achievements. The next generation of RFP experiments [13,35] with hotter plasmas will extend the data base toward reactor-relevant regimes of operation. The TITAN study has brought out and illuminated a number of key physics issues, some of which require greater attention from the RFP physics community. These issues are discussed in detail in Section 8.

The physics of confinement scaling, plasma transport, and the role of the conducting shell are already major efforts in RFP research. However, the TITAN study points to three other major issues. First, operating high-power-density fusion reactors with intensely radiating plasmas is crucial. Confirming that the global energy confinement time remains relatively unaffected while core-plasma radiation increases (a possible unique feature of RFP) is extremely important. Second, the TITAN study has adopted the use of three "open-geometry" toroidal divertors as the impurity control and particle exhaust system. Even with an intensely radiative plasma, using an array of poloidal pump-limiters as the impurity-control system would suffer from the serious erosion of the limiter blades (and possibly the first wall). The physics of toroidal-field divertors in RFPs must be examined, and the impact of the magnetic separatrix on RFP confinement must be studied. If toroidal divertors are consistent with confinement and stability in RFPs, then high-recycling divertors and the predicted high-density, low-temperature scrape-off layer must be also confirmed. Third, early work in the TITAN study convinced the team that high mass-power-density, compact RFP reactors must operate at steady state. Current drive by magnetic-helicity injection utilizing the natural relaxation process in RFP plasma is predicted to be efficient [9,10] but experiments on oscillating-field current drive (OFCD) are inconclusive. Testing OFCD in higher temperature plasmas must await the next generation of RFP experiments, namely ZTH [13] and RFX [35].

The key engineering issues for the TITAN-I FPC have been discussed. In the area of materials, more data on irradiation behavior of V-3Ti-1Si, especially irradiation-induced swelling, are needed to confirm the materials prediction and to estimate accurately the lifetime of the TITAN-I first wall. Further creep-rupture experiments are also needed to develop more precise creep-rupture models for V-3Ti-1Si. Compatibility of vanadium-base alloy with lithium coolant and the effects of a bimetallic loop also require more experimental data. Ceramic insulators offer the potential of minimum irradiation-induced

conductivity, high melting and decomposition temperature, retention of strength, and minimum irradiation-induced swelling. Further experimental data on irradiation behavior of these insulators are needed.

The low value of the toroidal field in the RFP allows high coolant velocities to be achieved without prohibitive MHD pressure drops, thus permitting operation in the turbulent-flow regime, with the associated high heat-transfer coefficients. Further experimental data on turbulent-flow heat-transfer capability of liquid metals, especially in the TITAN-relevant operational regime of low magnetic field and high velocities, are crucial to verify the TITAN-I thermal-hydraulic design. The combined effect, if any, of the parallel and perpendicular magnetic fields on flow transition and turbulent-flow heat transfer should also be investigated. The MHD pressure drop equations for bend, contraction, and a varying magnetic field need to be substantiated by further large-scale experiments and numerical and theoretical analyses. The effect of nonuniform heat flux on the heat-transfer capability (or Nusselt number) and volumetric nuclear heating in the coolant on the film temperature drop should be further studied.

The TITAN-I poloidal-field-coil system requires little or no extrapolation of current technology. But, the TITAN-I TF and divertor IBC design encounters several critical engineering issues. The most critical issue is the design of low-voltage, high-current power supplies for these coils. The requirement of oscillating voltages and currents for the OFCD compounds the IBC power-supply issues. The copper-coil option for both TF and divertor coils, similar to the TITAN-II design, is also possible.

The design of the impurity-control system poses some of the most severe problems of any component of a DT fusion reactor, and for a compact or high-power-density design these problems can be particularly challenging. Physics operation of high-recycling toroidal-field divertors in RFPs should be experimentally demonstrated and the impact of OFCD on the divertor performance studied. Cooling of the TITAN-I divertor plate requires experimental data on turbulent-flow heat transfer in liquid-metal systems, as outlined above. Fabrication of the tungsten divertor plate remains to be demonstrated and the degree of precision needed for target shaping and control of the position of the plasma separatrix are particularly difficult tasks.

The TITAN-I molten-salt tritium-recovery process needs large-scale demonstration. Any fusion reactor with vanadium first walls may encounter the problem of plasma-driven permeation (PDP) of tritium. The extent of PDP should be experimentally investigated.

The TITAN-I design uses many safety-design features to achieve a high level of safety assurance. Further detailed analysis of the response of the TITAN-I FPC to loss-of-

flow and loss-of-coolant accidents, including lithium fires, are needed to confirm the findings. Data are needed on elevated temperatures of vanadium alloys such as the recrystallization temperature, the onset temperatures and the extent of volatilization of radioactive products in vanadium, and the formation and release of vanadium oxide, V_2O_5 . In addition, in order to qualify for Class-C waste disposal, some of the impurity elements (mainly niobium and possibly silver, terbium, and iridium) need to be controlled in the vanadium alloy to below ppm levels.

In summary, the results from the TITAN study support the technical feasibility, economic incentive, and operational attractiveness of compact, high-mass-power-density RFP reactors. It must be emphasized, nevertheless, that in high-power-density designs such as TITAN, the in-vessel components (*e.g.*, first wall and divertor plates) are subject to high surface heat fluxes and that their design remains the most difficult engineering challenge. Also, the RFP plasma itself must operate in the manner outlined: with toroidal-field divertors, with a highly radiative core plasma, and at steady state. Future research will determine if, in fact, the physics and technology requirements of TITAN-like RFP reactors are achievable.

REFERENCES

- [1] F. Najmabadi, N. M. Ghoniem, R. W. Conn, *et al.*, "The TITAN Reversed-Field Pinch Reactor Study, Scoping Phase Report," joint report of University of California Los Angeles, General Atomics, Los Alamos National Laboratory, and Rensselaer Polytechnic Institute, UCLA-PPG-1100 (1987).
- [2] R. W. Conn (chairman and editor), "Magnetic Fusion Advisory Committee Panel X Report on High Power Density Fusion Systems" (May 8, 1985).
- [3] J. Sheffield, R. A. Dory, S. M. Cohn, J. G. Delene, L. F. Parsley, *et al.*, "Cost Assessment of a Generic Magnetic Fusion Reactor," Oak Ridge National Laboratory report ORNL/TM-9311 (1986) 103.
- [4] R. A. Krakowski, R. L. Miller, and R. L. Hagenon, "The Need and Prospect for Improved Fusion Reactors," *J. Fusion Energy* **5** (1986) 213.
- [5] R. A. Krakowski, R. L. Hagenon, N. M. Schnurr, C. Copenhaver, C. G. Bathke, R. L. Miller, and M. J. Embrechts, "Compact Reversed-Field Pinch Reactors (CRFPR)," *Nuclear Eng. Design/Fusion* **4** (1986) 75.
- [6] H. A. Bodin, R. A. Krakowski, and O. Ortolani, "The Reversed-Field Pinch: from Experiment to Reactor," *Fusion Technol.* **10** (1986) 307.
- [7] R. L. Hagenon, R. A. Krakowski, C. G. Bathke, R. L. Miller, M. J. Embrechts, *et al.*, "Compact Reversed-Field Pinch Reactors (CRFPR): Preliminary Engineering Considerations," Los Alamos National Laboratory report LA-10200-MS (1984).
- [8] C. Copenhaver, R. A. Krakowski, N. M. Schnurr, R. L. Miller, C. G. Bathke, *et al.*, "Compact Reversed-Field Pinch Reactors (CRFPR)," Los Alamos National Laboratory report LA-10500-MS (1985).
- [9] M. K. Bevir and J. W. Gray, "Relaxation, Flux Consumption and Quasi Steady State Pinches," *Proc. of RFP Theory Workshop*, Los Alamos, NM, U. S. A. (1980), Los Alamos National Laboratory report LA-8944-C (1982) 176.
- [10] K. F. Schoenberg, J. C. Ingraham, C. P. Munson, *et al.*, "Oscillating-Field Current-Drive Experiments in a Reversed-Field Pinch," *Phys. Fluids* **8** (1989) 2285; also R. A. Scardovelli, R. A. Nebel, and K. A. Werley, "Transport Simulation of the Oscillating Field Current Drive Experiment in the Z-40M," Los Alamos National Laboratory report LA-UR-2802 (1988).

- [11] J. B. Taylor, "Relaxation and Magnetic Reconnection in Plasma," *Rev. Mod. Phys.* **58** (1986) 741; also "Relaxation of Toroidal Plasma and Generation of Reversed Magnetic Fields," *Phys. Rev. Lett.* **33** (1974) 1139; and "Relaxation of Toroidal Discharges," *Proc. 3rd Topical Conf. on Pulsed High-Beta Plasmas*, Abingdon (September 1975), Pergamon Press, London (1976) 59.
- [12] M. M. Pickrell, J. A. Phillips, C. J. Buchenauer, T. Cayton, J. N. Downing, A. Haberstich, *et al.*, "Evidence for a Poloidal Beta Limit on ZT-40M," *Bull. Am. Phys. Soc.* **29** (1984) 1403.
- [13] P. Thullen and K. Schoenberg (Eds.), "ZT-H Reversed-Field Pinch Experiment Technical Proposal," Los Alamos National Laboratory report LA-UR-84-2602 (1984) 26.
- [14] D. Steiner, R. C. Block, and B. K. Malaviya, "The Integrated Blanket-Coil Concept Applied to a Poloidal Field and Blanket Systems of a Tokamak," *Fusion Technol.* **7** (1985) 66.
- [15] D. L. Smith, B. A. Loomis, and D. R. Diercks "Vanadium-Base Alloys For Fusion Reactor Applications – A Review," *J. Nucl. Mater.* **135** (1985).
- [16] D. L. Smith, G. D. Morgan, M. A. Abdou, C. C. Baker, J. D. Gordon, *et al.*, "Blanket Comparison and Selection Study – Final Report," Argonne National Laboratory report ANL/FPP-84-1 (1984).
- [17] E. E. Bloom, "Mechanical Properties of Materials in Fusion Reactor First-Wall and Blanket Systems," *J. Nucl. Mater.* **85-86** (1979) 795.
- [18] N. M. Ghoniem and R. W. Conn, "Assessment of Ferritic Steels for Steady State Fusion Reactors," *Fusion Reactor Design and Technology II*, International Atomic Energy Agency, IAEA-TC-392-62 (1983) p. 389.
- [19] M. E. Sawan and P. L. Walstrom, "Superconducting Magnet Radiation Effects in Fusion Reactors," *Fusion Technol.* **10** (1986) 741.
- [20] W. W. Engle, Jr., "A User's Manual for ANISN, A One-Dimensional Discrete Ordinates Transport Code with Anisotropic Scattering," Oak Ridge Gaseous Diffusion Plant report K-1693 (1967).
- [21] R. MacFarlane, "Nuclear Data Libraries from Los Alamos for Fusion Neutronics Calculations," *Trans. Am. Nucl. Soc.* **36** (1984) 271.

- [22] J. F. Briesmeister (Ed.), "MCNP – A General Monte Carlo Code for Neutron and Photon Transport, Version 3A," Los Alamos National Laboratory report LA-7396-M, Rev. 2 (1986).
- [23] D. S. Kovner, E. Yu. Krasilnikov, and I. C. Panevin, "Experimental Study of the Effects of a Longitudinal Magnetic Field on Convective Heat Transfer in a Turbulent Tube Flow of Conducting Liquid," *Magnitnaya Gidrodinamika* **2** (1966) 101.
- [24] R. A. Gardner and P. S. Lykoudis, "Magento-fluid-mechanics Pipe Flow in a Transverse Magnetic Field, Part 2, Heat Transfer," *J. Fluid Mech.* **48** (1971) 129.
- [25] E. Yu. Krasilnikov, "The Effect of a Transverse Magnetic Field upon Convective Heat Transfer in Magnetohydrodynamic Channel Flow," *Magnitnaya Gidrodinamika* **1** (1965) 37.
- [26] G. J. DeSalvo and J. A. Swanson, "ANSYS User's Manual," Swanson Analysis Systems, Inc. (1979).
- [27] L. C. Fuller and T. K. Stovall, "User's Manual for PRESTO: A Computer Code for the Performance of Regenerative Superheated Steam-Turbine Cycles," Oak Ridge National Laboratory report ORNL-5547, NASA CR-159540 (1975).
- [28] V. A. Maroni, R. D. Wolson, and G. E. Staahl, *Nucl. Technol.* **25** (1975) 83.
- [29] P. J. Burns, "TACO2D – A Finite Element Heat Transfer Code," Lawrence Livermore National Laboratory report UCID-17980, Rev. 2 (1982).
- [30] J. P. Holdren *et al.*, "Summary of the Report of the Senior Committee on Environmental, Safety and Economic Aspects of Magnetic Fusion Energy," Lawrence Livermore National Laboratory report UCRL-53766-Summary (1987); also J. P. Holdren *et al.*, "Exploring the Competitive Potential of Magnetic Fusion Energy: The Interaction of Economics with Safety and Environmental Characteristics," *Fusion Technol.* **13** (1988) 7.
- [31] S. J. Piet, "Approaches to Achieving Inherently Safe Fusion Power Plants," *Fusion Technol.* **10** (1986); also "Inherent/Passive Safety For Fusion," in *Proc. 7th ANS Topical Meeting on Tech. of Fusion Energy*, Reno, Nevada (1986).
- [32] F. M. Mann, "Transmutation of Alloys in MFE Facilities as Calculated by REAC (A Computer Code for Activation and Transmutation Calculations)," Hanford Engineering and Development Laboratory report HEDL-TME 81-37 (1982).

- [33] "Standards for Protection Against Radiation," U. S. Nuclear Regulatory Commission, Code of Federal Regulations, Title 10, Part 0 to 199 (1986).
- [34] S. Fetter, E. T. Cheng, and F. M. Mann, "Long-term Radioactivity in Fusion Reactors," *Fusion Eng./Des.* **6** (1988) 123.
- [35] G. Malesani and G. Rostagni, "The RFX Experiment," *Proc. 14th Symp. Fusion Technology*, Avignon (1986) 173.